University of Alberta

The Biochemical Characterization of the ATPase activity of three Hsp82 point mutants: Hsp82p^{A587T}, Hsp82p^{G313S}, and Hsp82p^{E381K}

by

BaoChan N. Mai

A thesis submitted to the Faculty of Graduate Studies and Research
in partial fulfillment of the requirements for the degree of

Master of Science

Department of Cell Biology

Fall 2012
Edmonton, Alberta

Abstract

Chaperones are family of proteins that assist in protein folding. 90 kDa Heat shock protein (Hsp90 mammalians, Hsp82 in *Saccharomyces cerevisiae*) is a well conserved chaperone that is essential for eukaryotic viability. The Hsp90 cycle is regulated by the ability to hydrolyze ATP, and through the interactions with other proteins known as co-chaperones. I biochemically characterized three Hsp82 point mutants: Hsp82p^{A587T}, Hsp82p^{G313S}, and Hsp82p^{E381K}, using co-chaperones known to influence the ATPase activity of Hsp82p (Aha1p, Sti1p, Sba1p, and Hch1p). The ATPase activity of the Hsp82p^{G313S} mutant could not characterize due to the low signal to noise ratio. I discovered the Hsp82p^{A587T} mutant ATPase activity was over stimulated by Aha1p, but had a similar relationship as the wild-type in terms of the Sti1p and Sba1p. With the Hsp82p^{E381K} mutant, I observed that the mutant was not stimulated robustly by Aha1p, and this stimulated rate was not inhibited by Sti1p.

TABLE OF CONTENTS

LIST OF TABLES

LIST OF FIGURES

Abbreviations

A	Alanine
ADP	Adenosine diphosphate
Aha1	accelerator of Hsp90 ATPase
Ahsa1	human accelerator of Hsp90 ATPase
Amp	ampicillin
APS	ammonium persulphate
ATP	adenosine triphosphate
Cdc37	Cell division 37
CNS1	cyclophilin seven suppressor 1
Cpr6	cyclosporin-sensitive proline rotamase 6
DMSO	dimethyl sulfoxide
dNTP	deoxyribonucleotide triphosphate
DTT	dithiothreitol
E	glutamate
EDTA	ethylenediamine-tetraacetic acid
EtBr	ethidium bromide
FRET	fluorescence resonance energy transfer
G	glycine
GF	gel filtration chromatography
GR	glucocorticoid receptor

Grp94	94 kDa glucose-regulated protein
Hch1	high copy suppressor of Hsp82
HCl	hydrochloric acid
HEPES	4-(2-hydroxyethyl)-1-piperazineethanesulfonic acid
HIC	hydrophobic interaction chromatography
HOP	Hsp70/Hsp90 organizing protein
Hsc82	constitutive form of yeast 82 kDa heat shock protein
Hsp	40 kDa heat shock protein
Hsp70	70 kDa heat shock protein
Hsp82	82 kDa inducible form of yeast heat shock protein
Hsp90	90 kDa human heat shock protein
Hsp90α	inducible form of human 90 kDa heat shock protein
Hsp90β	Constitutive form of 90 kDa human heat shock protein
HtpG	Heat shock protein htpG (Prokaryotic homologue)
IEX	ion exchange chromatography
IMAC	immobilized metal ion absorption chromatography
IPTG	isopropyl-beta-thiogalactopyranoside
K	lysine
kDa	kilodalton

LB	luria broth
LDH	lactate dehydrogenase
MCL	multiple cloning site
NAD^+	oxidized form of nicotinamide adenine dinucleotide
NADH	reduced form of nicotinamide adenine dinucleotide
p23	23 kDa proteolytically resistant protein
PBS	phosphate buffered saline
PCR	polymerase chain reaction
PEP	phosphoenolpyruvate
PK	pyruvate kinase
PP5	phosphoprotein phosphates 5
PPIase	peptidyl-prolyl cis-trans isomerise
PR	progesterone receptor
S	serine
S. cerevisae	*saccharomyces cerevisiae*
Sba1	increased sensitivity to benzoquinone ansamycins 1
SDS	sodium dodecyl sulfate
SSF1	suppressor of ste4 1
Sti1	stress inducible
T	tyrosine
TEMED	tetramethylethylenediamine

TPR	tetratricopeptide repeat
ts	temperature sensitive
UV	ultraviolet
WHMIS	workplace hazardous materials information sheet
WT	wild-type

Chapter 1

Introduction

1.1 Overview

The acquisition of a proper three dimensional structure is crucial for the functional role a protein will play in the cell. In the 1960's, Christian Anfinsen demonstrated that the information required for protein folding is dictated by the primary sequence of protein [1]. In very dilute solutions where intermolecular interactions are unlikely to occur, intramolecular interactions between the hydrophobic and hydrophilic amino acid side chains of the polypeptide chain drive protein folding. In vivo, where the protein concentration in a cell is high, intermolecular interactions with other polypeptide chains are more likely to occur and interfere with protein folding. When polypeptide chains interact intermolecularly, many of these interactions will result in aggregation and loss of proper function of the protein [2,3,4]. Because of the importance of folding for protein function, the cell utilizes a class of proteins that are collectively known as chaperones to prevent intermolecular interactions**.** Chaperones assist in protein folding by utilizing different mechanisms to stabilize both the protein and intermediate structures and prevent inappropriate intermolecular interactions from occurring. This study focuses on a specific chaperone called the 90 kDa heat shock protein (Hsp90).

1.2 Hsp90

Hsp90 is a well conserved, homodimeric chaperone that is found in prokaryotes and eukaryotes, although it is absent in archaea. The chaperone is essential for eukaryotic cell viability [3,5,6]. Hsp90 comprises as much as 2% of

the cellular protein in an unstressed cell and its expression is upregulated during times of stress [7,8]. In addition to cytoplasmic Hsp90, higher eukaryotes have paralogs in the endoplasmic reticulum (Grp94), and mitochondria (Trap1)**.** Eukaryotes have two forms of cytoplasmic Hsp90; one form is constitutively expressed (Hsp90β, human; Hsc82, *Saccharomyces cerevisae*), and another that is inducible during times of stress (Hsp90α, human; Hsp82, *S. cerevisae*). Hsp90 is well conserved from species to species, with the constitutive and inducible form being nearly identical within species [5,9,10].

The primary function of Hsp90 in the cell is to assist in the maturation of specific substrates known as 'client' proteins. Unlike many other classes of chaperones, including Hsp70/Hsp40, Hsp90 does not bind to client proteins in their unfolded state by recognizing non-specific, exposed hydrophobic residues [11]. Instead, the client proteins that interact with Hsp90 are already in a folded or partially folded state [12]. This property is unique to Hsp90, and presumably occurs through the recognition of a specific, but currently unidentified, element of secondary or tertiary structure found in its client proteins [5,13,14,15]. Though Hsp90 interacts with a specific subset of client proteins, these client proteins are very diverse in their structure and function, and are known to be involved in many different biological processes including cell signalling, protein transcription, and transport [16,17,18,19]. Many Hsp90 client proteins are oncoproteins, which require Hsp90 for their stabilization, and/or activation. For this reason Hsp90 is often referred to as a 'master regulator' in cancer [20,21]. Due to the dependency

that transformed cancer cells have on Hsp90, understanding Hsp90 function and mechanism will allow for insight into oncogenesis.

As previously mentioned, Hsp90 is very well conserved, and the structure has been extensively studied. Hsp90 is composed of four domains: the N-terminal domain, a charged linker, middle domain and a C-terminal domain (Figure 1.1) [9,22,23,24]. Hsp90 exists as a homodimer, with dimerization of the Hsp90 monomers occurring at the C-terminal domain. The C-terminal dimerization is essential for the activity of Hsp90, and the dimerization constant for wild-type yeast Hsp90 is 60 nM, [25,26]. At the end of the C-terminus is a highly conserved pentapeptide (MEEVD) that is also found in other chaperone families, such as Hsp70 [27,28,29]. The MEEVD peptide is important for binding to other proteins such as the Hsp70/Hsp90 organizing protein [30] [31,32,33]. The middle domain is the interface where client proteins interact with Hsp90 [34,35]. Between the middle and N-terminus, there is a largely unstructured, highly charged linker domain. This domain allows for flexibility of the Hsp90 dimer, but the length and sequence is very diverse between different species. Recently, the sequence of the charged domain has been demonstrated to play a more important role on ATP and client binding properties then the actual length of the linker domain [36,37]. The N-terminal domain of Hsp90 is where ATP is bound and hydrolyzed. The ATP binding pocket of Hsp90 is unique compared to other ATPases, which is useful when studying the chaperone as inhibitors that are highly specific to Hsp90 exist [22,23].

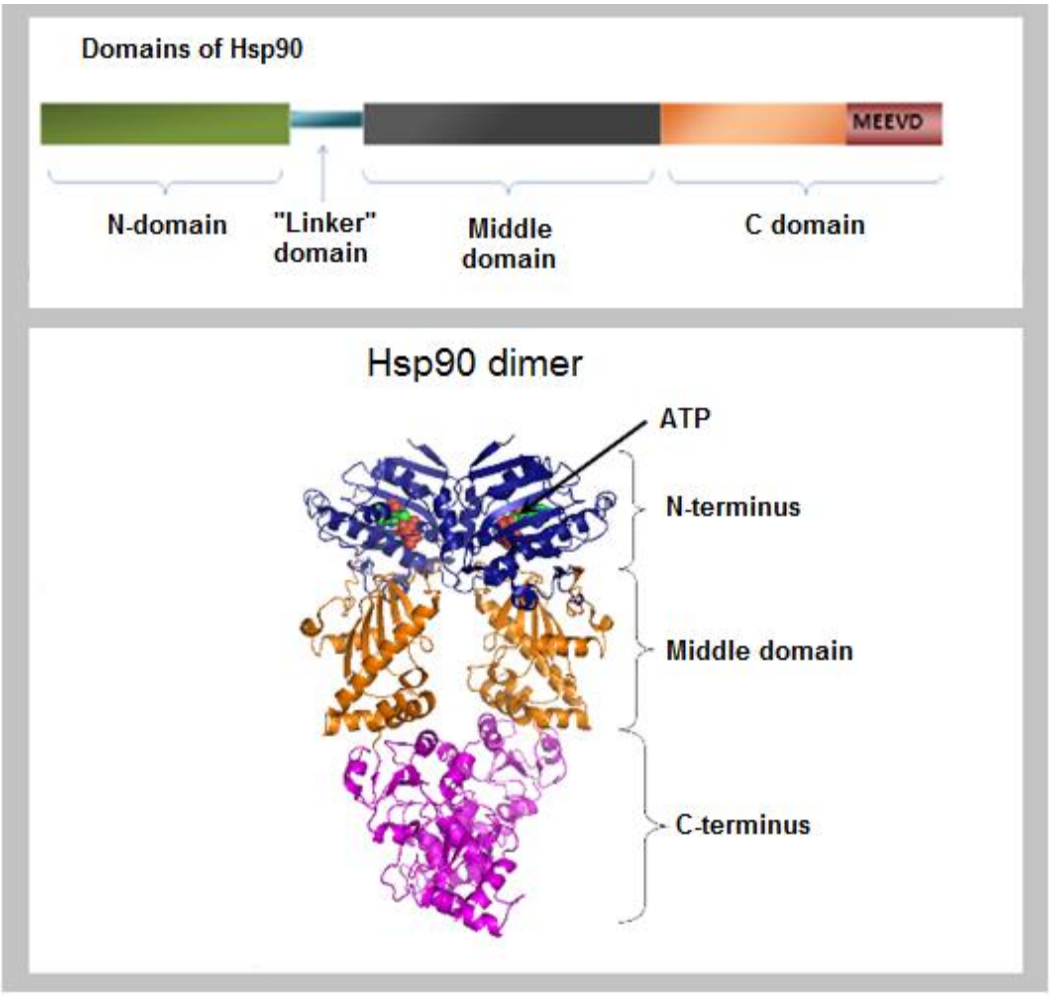

FIGURE 1.1: Diagram of domains and ribbon structure of the dimeric Hsp90

A schematic diagram of the domains of Hsp90 (upper panel). Below is a ribbon structure of an Hsp90 dimer bound to ATP (lower panel).

The structure of the homodimeric unit of Hsp90 is very dynamic and known to transition between closed and open forms [38,39,40] (Figure 1.2). It was previously thought that the conformation of Hsp90 is dictated by nucleotide binding and hydrolysis [41,42]. The closed conformation is induced when ATP molecules bind to the N-terminus of Hsp90. The binding of ATP triggers the N-terminus of each monomer to move closer together. This dimerization of the N-terminus results in the formation of a "lid" and hydrolysis of ATP occurs. After the hydrolysis of ATP, the N-termini move apart, ADP is released, and the chaperone adopts an open conformation. More recently, Ratzke *et. al* suggested that the Hsp90 conformation is dictated by ATP binding and hydrolysis is overly simplified [42]. Using fluorescence resonance energy transfer (FRET) technology, it was demonstrated that both the open and closed forms of Hsp90 were capable of binding ATP and ADP. The rate at which ATP binds and is released is also much faster than the rate of hydrolysis; this implies that ATP binding is not necessarily followed by hydrolysis [5,12,43,44,45,46,47].

1.3 Introduction to the Hsp90 cycle

Though the structure of Hsp90 has been thoroughly dissected, the mechanism by which Hsp90 aids in the maturation of client proteins is still unclear. To a large extent what is known about how Hsp90 interacts with client proteins was derived from studies that looked at the client progesterone receptor (PR) and glucocorticoid receptor (GR) proteins. From these studies we know that in order to promote folding and activation of its client proteins, Hsp90 must move

through a dynamic and transient multi-chaperone cycle. The progression through the cycle is regulated by proteins known as co-chaperones (Figure 1.3) [5,48,49].

Many co-chaperone proteins are highly conserved and functionally interchangeable between species. Some co-chaperones are essential, while others can be deleted with no effect on cell viability [51]. The co-chaperones of cytosolic Hsp90 can be roughly categorized into two main groups: Tetratricopeptide repeat (TPR) and non-TPR co-chaperones [52]. TPR co-chaperones recognize and bind to the conserved MEEVD motif on the C-terminus of the Hsp90 dimer. Many of these TPR co-chaperones contain other domains that are involved in different biological functions that may assist Hsp90 directly or indirectly in the maturation of client proteins. An example is phosphoprotein phosphatase 5 (PP5); PP5 is a TPR co-chaperone that contains a serine phosphatase domain, and has been shown to be important for mediating interaction between GR and Hsp90 [53]. All other co-chaperones that do not recognize and bind to the MEEVD domain can be categorized as non-TPR co-chaperones, and are very diverse in their structure and function. An example of a non-TPR co-chaperone is cell division 37 (Cdc37); Cdc37 is an essential co-chaperone that is important for the stabilization of Hsp90-kinase complexes [27,28,39,54]. Clearly co-chaperones play an important role in influencing the function of Hsp90, and by understanding their relationship with the chaperone we hope to gain further insight into the complexity of the Hsp90 cycle.

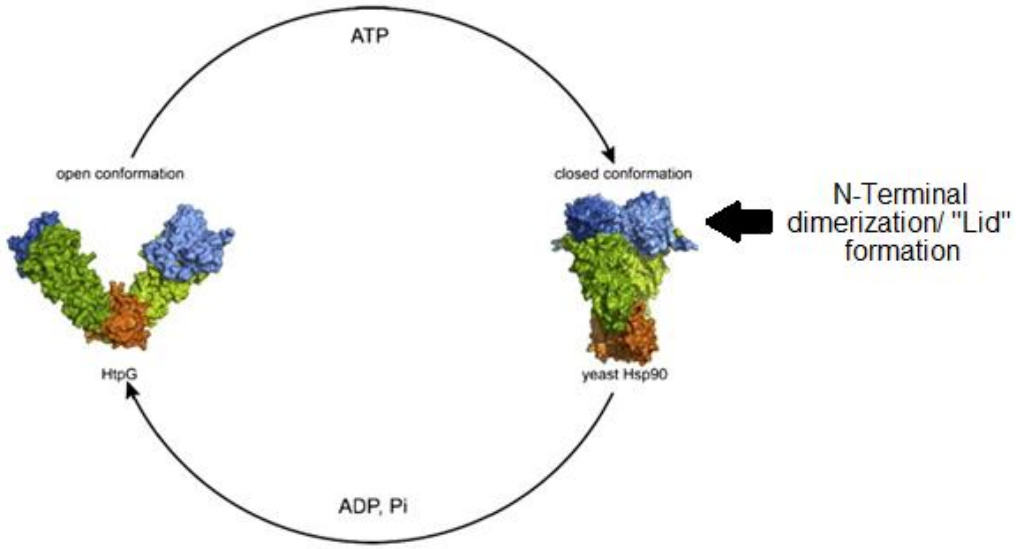

FIGURE 1.2: Model of the open and closed conformations of the Hsp90 dimer

Hsp90 modeled on the prokaryotic homologue HtpG and yeast Hsp82p. The domains of Hsp90 are depicted: N-terminus (blue), Middle domain (green) and C-terminus (orange). The open conformation based on *E. coli* HtpG (left), and the closed ATP bound conformation of *S. cerevisae* Hsp82p. Modified figure from reference [50].

The Hsp90 system between yeast and mammalians are highly conserved (Table 1.1). In this study, the inducible yeast Hsp82 and yeast co-chaperones were used to study the Hsp90 chaperone system. For reference, the notation of Hsp90 is used to discuss the chaperone system in a generic sense, while the notation of Hsp82 and the specific co-chaperones is used when referring to my study in detail.

1.3.1 "Early stage" of Hsp90 cycle - Sti1p

The Hsp70/Hsp90 organizing protein (Hop in mammals, and Sti1p in *S. cerevisae*) is one of the first co-chaperones to interact with Hsp90 (Figure 1.3, Step 1). Sti1p has nine tetratricopeptide repeat (TPR) motifs that form three (TPR1, TPR2A and TPR2B) 'carboxylate clamp' binding pockets [28,39]. Studies of the structure have shown that the basic amino acids in the carboxylate clamp are able to form a salt bridge with acidic amino acids in the conserved pentapeptide domain (MEEVD) [28]. Sti1p is able to interact with both Hsp90 and Hsp70 independently or simultaneously. The Hsp90 C-terminus has been shown in crystal structures to bind specifically to TRP2A, while Hsp70 C-terminus binds to the TPR1 domain of Sti1p [5,12,45,55].

The ability of Sti1p to bind simultaneously to both MEEVD regions in Hsp70 and Hsp90 allows for Sti1p to bring chaperone systems in close proximity - essentially tethering the Hsp90 and Hsp70/Hsp40 chaperone system together.

This allows for the exchange of a partially folded client protein from the Hsp70 system to the Hsp90 system for further maturation. The loading of the client onto Hsp90 signals the start of a new cycle for the system [56].

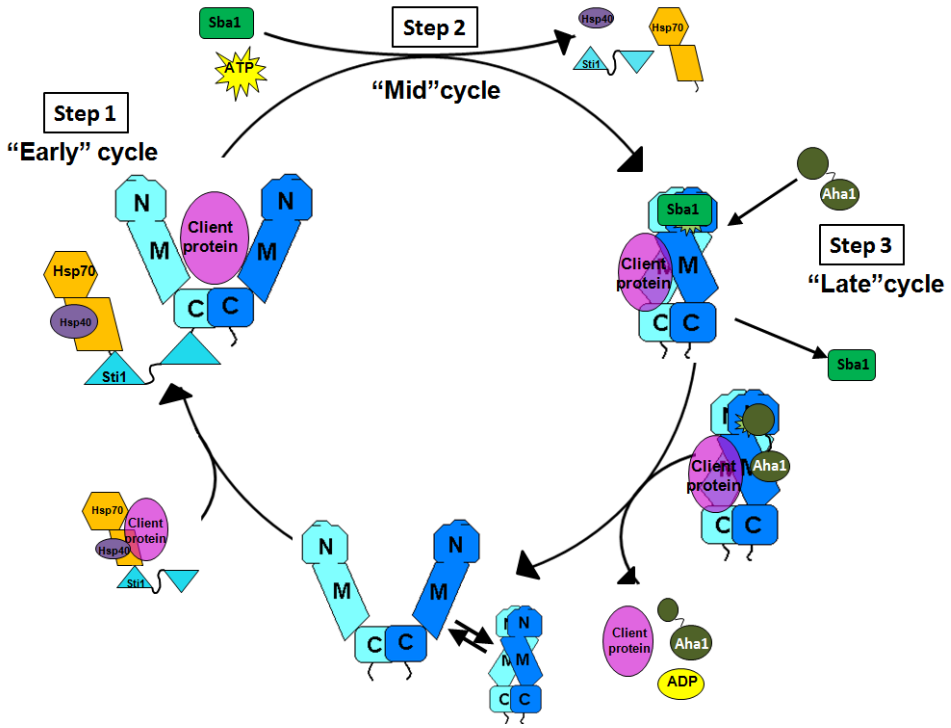

FIGURE 1.3: Theoretical model of Hsp90 cycle

(Step 1) The "early" stages of the Hsp90p cycle has to do with client transfer. Sti1p binds to the MEEVD motif on the C-terminus of Hsp90. Sti1p is also bound to an earlier chaperone system (Hsp40/70) that has already assisted the client protein in its' folding. Sti1p tethers both the Hsp40/70 and Hsp90 system in close proximity to each other, and facilitates client transfer. **(Step 2)** The "mid" cycle of the Hsp90 is marked by the binding of Sba1p and ATP. The binding of Sba1 and ATP displaces Sti1p allowing Hsp90 to adopt and N-terminal dimerization/closed conformation. **(Step 3)"** Late" in the cycle, Aha1p binds to Hsp90. This results in the displacement of Sba1p, promoting the hydrolysis of ATP, and client protein release. At the end of the cycle Hsp90 dimer is then free to adopt the open or closed conformation and start the cycle again.

The binding of Sti1p to Hsp90 promotes the open ADP bound conformation, and significantly inhibits Hsp90 ATPase activity by preventing the conformational changes required for N-terminal dimerization [57]. Sti1p effectively inhibits the ATPase activity of Hsp90, by preventing N-terminal dimerization, which is necessary for the loading of client proteins [58]. Only one Sti1p molecule is necessary to inhibit the ATPase of an Hsp90 dimer [29,58,59,60].

1.3.2 "Intermediate stages" of Hsp90 cycle – Sba1p

After Sti1p has facilitated the transfer of client from the Hsp70/Hsp40 system to Hsp90, the next step involves the binding of an intermediate co-chaperone: Sba1p in *S. cerevisae* (p23 in mammalian cells).

Sba1p favors binding to Hsp90 in the closed ATP-bound conformation, and is known to inhibit Hsp90 ATPase activity to a lesser extent than Sti1p [29]. Crystallographic studies have shown that the Sba1p monomer interacts with the middle and the N-terminus of Hsp90 (Figure 1.4). Binding of Sba1p displaces Sti1p, and promotes Hsp90 dimer to adopt a closed conformation which important for later steps in the Hsp90 cycle involving ATP hydrolysis [16,61,62,63]. The binding of Sba1p plays a critical role in the stabilization of the Hsp90-client complex [64,65] (Figure 1.3, Step 2). Aside from the role as an Hsp90 co-chaperone, independently, Sba1 also has its own chaperoning abilities. Similar to Hsp90, Sba1p holds proteins in a folding competent state by binding to a protein in a non-native state, and preventing thermal aggregation during times of stress [66,67].

TABLE 1.1: Summary of the components in the Hsp90 system

Yeast name	**Human name**	**% Identity**	**% Similarity**	**Description**
Hsc82	Hsp90β	61%	85%	Constitutively expressed form of Hsp90
Hsp82	Hsp90α	61%	84%	Stress-induced form of Hsp90
Sti1	Hop (STIP1)	36%	66%	Stress Inducible Phosphoprotein – Hsp90 co-chaperone Binds to MEEVD motif in the C-terminus of Hsp90 and other chaperones (ex.Hsp70) to facilitate the transfer of client proteins from one system to another.
Sba1	p23	21%	56%	Sensitivity to Benzoquinone Ansamycins –Hsp90 co-chaperone Interacts with Hsp90-client complex
Aha1	Ahsa1	23%	64%	Accelerator of Hsp90 ATPase activity - Hsp90 co-chaperone
Hch1	---	---	---	High Copy suppressor of Hsp82 (Hch1) –Hsp90 co-chaperone Homolog of Aha1 with no known functional relevance

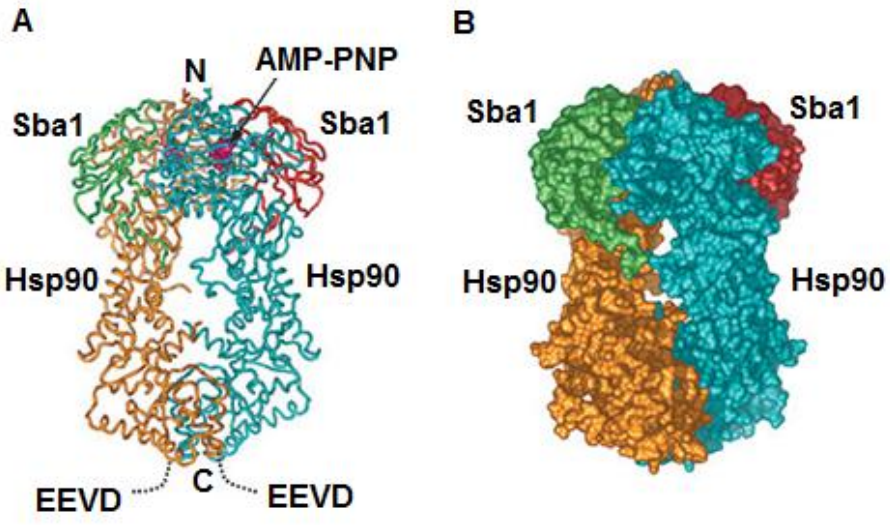

FIGURE 1.4: Crystal structure of Sba1p interacting with an Hsp90 dimer

(A) Amino acid backbone of Sba1p (green and red) bound to an Hsp90 dimer in a closed AMP-PNP bound conformation (blue and orange).

(B) The molecular surface of Sba1p (green and red) bound to an Hsp90 dimer in a closed AMP-PNP bound conformation (blue and orange). Modified figure from [68].

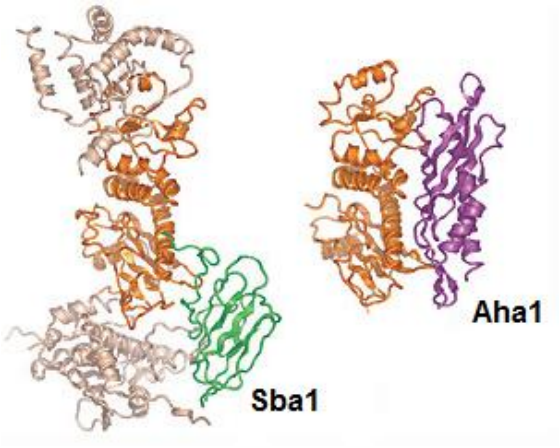

FIGURE 1.5: Binding of Sba1p and N-terminus of Aha1p overlap in the middle domain of Hsp90

Ribbon structure of a Hsp90 monomer (the C terminus and N terminus is (tan), Middle domain (orange)). Sba1p (green) interacts with the C-terminus and middle domain (tan and orange) of Hsp90 monomer (left). Aha1p (purple) interacts with the Middle domain (orange) of the Hsp90 monomer [69]. Modified figure from [68].

1.3.3 "Late stage" of Hsp90 cycle – Aha1p

One of the last steps in the Hsp90 cycle involves a co-chaperone as the Accelerator of Hsp90 ATPase activity known Aha1p in *S. cerevisae* (Ahsa1 *H. sapiens*). It is known from crystallographic studies that the N-terminus of Aha1p binds to the middle domain of Hsp90, and the C-terminus of Aha1p binds to the N-terminus of Hsp90. Aha1p preferentially binds to the closed, ATP-bound state of Hsp90, and acts to promote subsequent ATP hydrolysis. Aha1p is the only co-chaperone that robustly stimulates the low intrinsic ATPase rate of Hsp90. *In vitro* experiments showed that when Aha1p and Hsp90 are added in a 1:1 ratio, the intrinsic ATPase rate of Hsp90 was stimulated by ~5 to 12 fold [32,70]. This hydrolysis allows for the release of the client protein and transition back to the open conformation of the Hsp90 dimer for the loading of new client. (Figure 1.3, Step 3). Despite the significant effect that Aha1p has on the ATPase of Hsp90, Aha1p only improves the efficiency of the Hsp90 chaperone machine, but is not essential for its overall function [57,68].

Using gel filtration chromatography, Harst *et. al.* found that the binding of Sba1p and Aha1p to the Hsp90 dimer was mutually exclusive [57]. Crystal structures have shown that both Sba1p and Aha1p compete for the same region in the middle domain of Hsp90, due to the steric hindrance both co-chaperones cannot bind to the middle domain of Hsp90 at the same time (Figure 1.5) [57].

1.4 – A Novel co-chaperone - Hch1p

Hsp90 has another co-chaperone known as the High Copy suppressor of Hsp82 (Hch1p). Hch1p is a truncated homologue of Aha1 and is only found in

lower eukaryotes, including *S.cerevisae*. Hch1p is missing the 197 amino acids (aa) C-terminus that Aha1p contains, and shares 36.5% sequence identity to the N-terminus of Aha1p (Figure 1.6). Though Hch1p has never been crystallized, it is thought to bind to the same region in the middle domain on Hsp90 as Aha1p due to the conserved amino acid residues [71] . Hch1 was originally discovered in a screen performed in yeast, and its overexpression was found to suppress the temperature sensitive phenotype of an Hsp82p variant harbouring the E381K point mutation (Figure 1.7) [72]. Unlike Aha1p, Hch1p only weakly stimulates Hsp90 ATPase activity. *In vitro* experiments where Hch1p was added in a 1:1 ratio with Hsp90 did not stimulate the low intrinsic ATPase rate of Hsp90, as compared to a ~12 fold stimulation seen when the same experiment was performed with Aha1p. Hch1p was shown to only to weakly stimulate the low intrinsic ATPase rate of Hsp90 by ~3.5 fold, when the co-chaperone was added in excess (a 10:1 ratio) [57,73,74,75]. Hch1p is not well characterized in the field and is believed to have a redundant function to Aha1p due to the conservation of key residues between Aha1p and Hch1p, and the lack of *HCH1* in higher eukaryotes [6].

1.5 Studying mutant Hsp90 in yeast

Temperature sensitive (ts) mutants are used when studying Hsp90 because the chaperone is essential for cell viability [3]. In the yeast model system used to study the Hsp90 system, many temperature sensitive mutants are available [76].

(A)

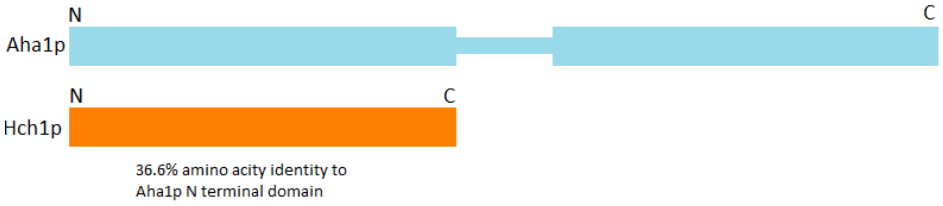

(B)

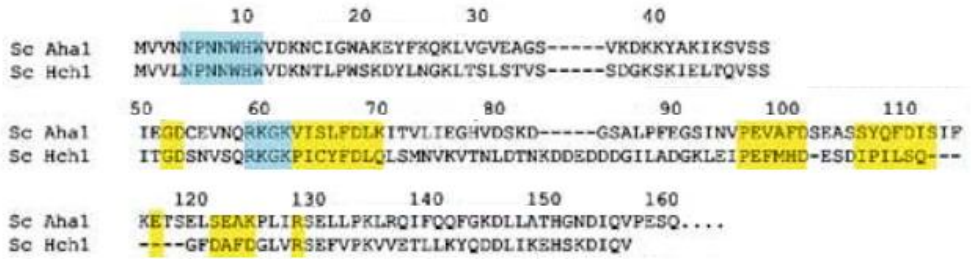

FIGURE 1.6: Schematic diagram of domains and alignment of Aha1p with Hch1p

(A) Schematic domain diagram of Aha1p (blue), and Hch1p (orange) (upper panel). **(B)** Alignment of N terminus of Aha1p (160 amino acids) and Hch1p (156 amino acids) amino acid sequence. The strongly conserved basic motifs are highlighted in blue, and the regions that come in contact with Hsp90 are highlighted in yellow. Modified figure from [71].

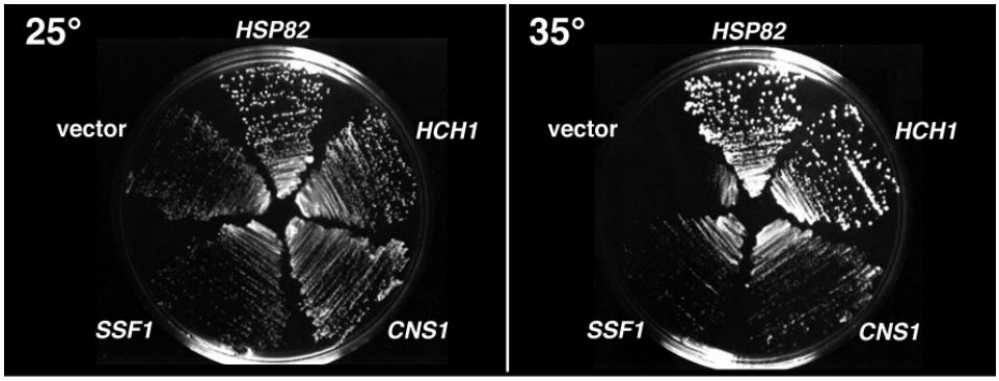

FIGURE 1.7: Overexpression of SSF1, CNS1, and HCH1 restores the growth yeast expressing $Hsp82^{E381K}$ at elevated temperatures

Yeast expressing $Hsp82^{E381K}$ as the sole source of Hsp90, and the TRP is transformed with a plasmid encoding a control vector (vector) , wild –type Hsp82p, Hch1p , Ssf1p, or Cns1p. These strains of yeast were grown at at permissive (25°C – left panel) and non-permissive temperatures (35°C- right panel) for three days on SD media lacking tryptophan. The over expression of wild –type Hsp82p, Hch1p , Ssf1p, or Cns1p resuce the temperature sensative growth defect of $Hsp82^{E381K}$ at 35°C. Figure from [76].

Many of these mutants are not "classical" temperature sensitive mutants in the sense that they become unfolded at non-permissive temperatures. Instead the point mutations used to study Hsp90, display temperature sensitive phenotypes as a result of their impaired activity being insufficient for the cellular needs at higher temperatures [2,31,72]. This implies that these mutants have unique molecular defects at different steps of the Hsp90 cycle that prevent it from functioning efficiently like the wild-type during times of increased stress. Of the many mutants, I focused on three for this study: Hsp82p^{E381K}, Hsp82p^{A587T}, and Hsp82p^{G313S} (Figure 1.8). By utilizing three different temperature sensitive mutants and deciphering their molecular defects, I hope to discover more about how Hsp90 functions at the different steps of the Hsp90 cycle (Figure 1.3).

I chose to further biochemically characterize three particular mutants, Hsp82p^{E381K}, Hsp82p^{A587T}, and Hsp82p^{G313S} based on their relationship with the Hch1p. Work done in the lab demonstrated that the deletion or overexpression of *HCH1* has different effects on Hsp82^{E381K}, Hsp82^{A587T}, and Hsp82^{G313S}. Nathan *et.al* were the first to identify Hch1p, and showed that the temperature sensitive defect of yeast expressing Hsp82^{E381K} was reversed by the overexpression Hch1p (Figure 1.7) [77,78]. Because Hch1p and the N-terminus of Aha1p share a high degree of sequence identity, we had hypothsized that we would see similar rescue in the growth phenotype of yeast expressing Hsp82p^{E381K} when Aha1p or the N-terminus of Aha1p (Aha1p$^{1-156}$) was overexpressed. To test this hypothesis, an experiment was carried out on yeast expressing Hsp82p^{E381K}, as well as over expressing one of the following proteins Hch1p, Aha1p, or Aha1p$^{1-156}$ (Figure

1.9). We found that only the over expression of Hch1p was able to rescue the growth defect of Hsp82p^{E381K}. This suggested that Hch1p had a function which was unique from Aha1p, and that this function rescued the molecular defect of Hsp82p^{E381K} so that the mutant could better cope with the increased stress on the system due to higher temperatures.

We also looked at the relationship between Hch1p and the other two mutants, Hsp82p^{A587T} and Hsp82p^{G313S}. We found that the deletion of Hch1p rescued yeast expressing Hsp82p^{A587T} and Hsp82p^{G313S} –the opposite effect that we saw with Hsp82p^{E381K} (Figure 1.10).

1.6 Focus of this thesis

From the observation seen in yeast expressing these mutants, I formed a two part hypothesis from which my thesis was based on. The first part of my hypothesis being that the defect of Hsp82p^{E381K} is rescued by the presence of Hch1p. The second is that the molecular defect of both Hsp82p^{A587T} and Hsp82p^{G313S} is exacerbated by the presence of Hch1p. Knowing that Hsp82p^{E381K}, Hsp82p^{A587T} and Hsp82p^{G313S} each have a unique molecular defect in the Hsp90 cycle, I wanted to utilize these mutants to discover where Hch1p affected the Hsp90 cycle.

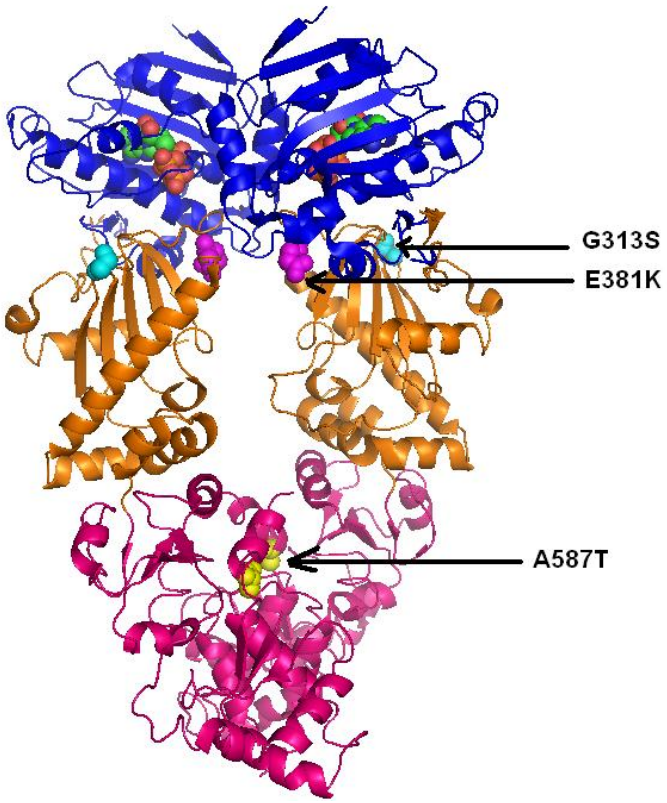

FIGURE 1.8: Ribbon structure of Hsp90 dimer bound to ATP with labelled sites of the mutations used in this study (Hsp82^{A587T}, Hsp82^{E381K}, and Hsp82^{G313S}) Ribbon structure of Hsp90 dimer: the N-terminus (dark blue), middle domain (orange) , C-terminus (magenta). Hsp82p dimer bound to ATP (green and red) showing the placement of the point mutations: Hsp82^{A587T} (yellow), Hsp82^{E381K} (light pink), and Hsp82^{G313S} (light blue).

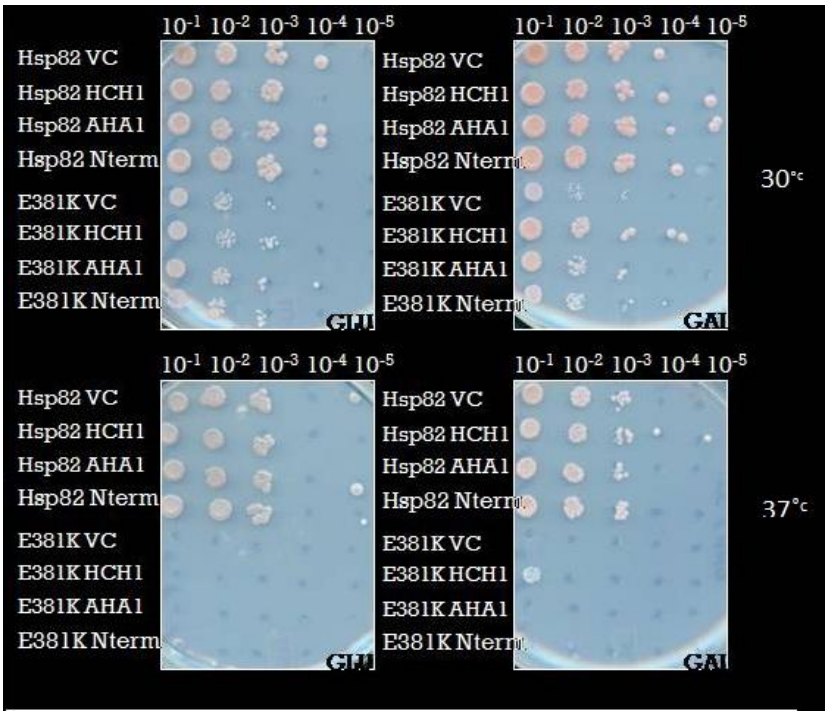

FIGURE 1.9: Effects of over-expression of *HCH1, AHA1* and the N-terminus of AHA1 (Aha1p$^{1-156}$) on the growth of Hsp82^{E381K} mutant

Growth assay with yeast expressing either the wild-type Hsp82p or the Hsp82p^{E381K} mutant. The yeast cells were transformed with plasmids encoding either: vector control (VC), *HCH1, AHA1* and Aha1p$^{1-156}$ (N-term) under the control of a Gal1 promoter. The strains were grown on SC-TRP-URA glucose (Left panels) or galactose media plates (Right panels) at permissive (30°C top panels) and restrictive temperatures (37°C bottom panels). Under the repressing conditions all yeast strains expressing Hsp82p^{E381K} show growth impairment at 30°C and 37°C (left panel). When the strains are grown in non-repressive conditions there is a rescue of growth with the yeast strains expressing Hsp82p^{E381K} when Hch1p is over expressed (right panel).

FIGURE 1.10: Effects of over-expression of *HCH1* on the growth of Hsp82^{A587T}, Hsp82^{G313S} mutant

(A) Growth assay with yeast expressing either the wild-type Hsp82p (WT) or the Hsp82p^{A587T} mutant. These yeast strains either had *HCH1*gene present (---) or deleted (Δ*hch1*), and were grown at permissive (30°C left panels) and restrictive temperatures (37°C right panels). Under the permissive conditions (30°C) all yeast strains grow similarly (left panel). Under non-permissive temperatures (37°C) the yeast strain expressing Hsp82p^{A587T} that had *HCH1*gene present (---) showed a growth impairment (bottom right panel), this impairment was rescued with the deletion of *HCH1* (Δ*hch1)* (bottom right panel).

(B) Growth assay with yeast expressing either the wild-type Hsp82p (WT) or the Hsp82p^{G313S} mutant. These yeast strains either had *HCH1*gene present (---) or deleted (Δ*hch1*), and were grown at permissive (30°C left panels) and restrictive temperatures (35.5°C right panels). Under the permissive conditions (30°C) all yeast strains grow similarly (left panel). Under non-permissive temperatures (35.5°C) the yeast strain expressing Hsp82p^{G313S} that had *HCH1*gene present (---) showed a growth impairment (bottom right panel), this impairment was rescued with the deletion of *HCH1* (Δ*hch1)* (bottom right panel).

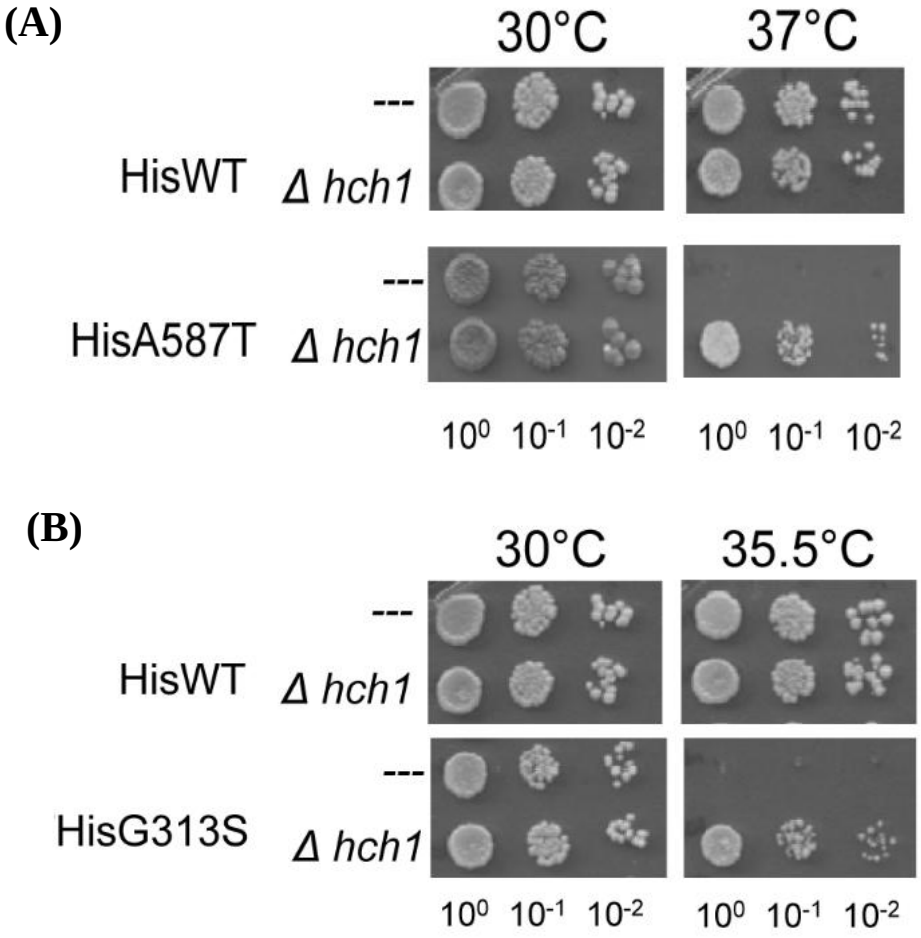
(A)
30°C
37°C

HisWT
Δ hch1

HisA587T
Δ hch1
10^0 10^-1 10^-2
10^0 10^-1 10^-2
(B)
30°C
35.5°C

HisWT
Δ hch1

HisG313S
Δ hch1
10^0 10^-1 10^-2
10^0 10^-1 10^-2

Before I could discover a novel function for Hch1p, I needed to characterize the step of the Hsp90 cycle at which Hsp82p^{E381K} was deficient so that I could observe if the presence of Hch1p was able to rescue the mutant at that particular step. On the other hand, I also needed to characterize how both Hsp82p^{A587T} and Hsp82p^{G313S} were similar to the wild-type, and observe if the presence of Hch1p adversely affected the mutants' ability to function.

For this study, I focused on biochemically characterizing the mutants' ATPase activity and the effects of different co-chaperones using purified yeast proteins (Table 1.1). The ATPase activity of Hsp90 plays an important role in the function of the chaperone. Like many other classes of chaperones, Hsp90 activity is driven by the ability to bind and hydrolyze ATP. The ATPase activity of the chaperone is essential; other studies have shown that yeast are not viable when expressing mutants that do not bind, or bind but cannot hydrolyze ATP [41]. Co-chaperone interactions with Hsp90 also influence binding, selection, and maturation of client proteins. Despite Hsp90 interacting with many different co-chaperones, in addition to Hch1p, I focused on three others: Sti1p, Sba1p, and Aha1p. It was important to study these three additional co-chaperones as they influence the ATPase activity of Hsp90, and interact with Hsp90 at different stages in the cycle (Figure 1.3).

Chapter 2

Materials and Methods

2.1 Materials

Tables 2.1- 2.3 below list the chemical, reagents, enzymes, and molecular kits used in this study. All the materials, chemicals and enzymes used in experimental procedures were molecular biology grade, and in accordance with the procedures set out by the Environmental Health and Safety of the University of Alberta and Workplace Hazardous Material Information System (WHMSIS).

TABLE 2.1: List of chemicals and reagents

Chemical	Company name
2-Mercaptoethanol (β-Mercaptoethanol)	Fisher Scientific
acetic acid, glacial	Fisher Scientific
acetone	Fisher Scientific
acrylamide/bis (30%; 29:1)	Bio-Rad
agarose (UltraPure^{TM})	Invitrogen
ammonium acetate ($NH_4(C_2H_3O_2)$)	Fisher
ammonium chloride (NH_4Cl)	Invitrogen
ammonium persulphate (APS)	BDH
ampicillin	Novopharm
bacto-yeast	BD
calcium chloride (CaCl)	BDH
complete, EDTA-free protease inhibitor cocktail tablets	Roche
chloroform	Fisher
dithiothreitol (DTT)	Fisher Scientific

dimethyl sulfoxide (DMSO)	Sigma
deoxyribonucleotide triphosphate (dNTP)	Invitrogen
ethidium bromide (EtBr)	Sigma
ethylenediamine-tetraacetic acid (EDTA)	Sigma
glycerol	Fisher Scientific
hydrochloric acid (HCl)	Fisher Scientific
4-(2-hydroxyethyl)-1-piperazineethanesulfonic acid (HEPES)	Invitrogen
isopropanol	Fisher Scientific
imidazole	Fisher Scientific
kanamycin	Sigma
magnesium chloride (MgCl)	BDH
magnesium sulphate ($Mg(SO_4)$)	Fisher Scientific
methanol	Fisher Scientific
ponceau S	Sigma
potassium chloride (KCl)	BDH
sodium bicarbonate ($NaHCO_3$)	Caledon
sodium chloride (NaCl)	Fisher Scientific
sodium dodecyl sulfate (SDS)	Bio-Rad
sodium hydroxide (NaOH)	Fisher Scientific
sodium sulphate Na_2SO_4	Sigma
tetramethylethylenediamine (TEMED)	BioRad
Tween 20 (polysorbate 20)	Fisher Scientific

TABLE 2.2: List of enzymes

Enzyme name	Company name
DNA ligase T4	Invitrogen or NEB
Nde1	Fermentas
BamH1	Fermentas
LDH (Lactate Dehydrogenase)	Sigma
PK (Pyruvate Kinase)	Sigma
TopTaq	Qiagen

TABLE 2.3: List of molecular biology kits

Molecular Kit	Company name
QIAprep Miniprep Kit	Qiagen
QIAprep Midiprep Kit	Qiagen
QIAquick Gel Extraction Kit	Qiagen
QuikChange™ Site-Directed Mutagenesis Kit	Stratagene
DNA T4 ligase kit	NEB

2.2 Molecular size standards

The molecular weight standard run on agarose gels was GeneRuler™ 1 Kb DNA Ladder. The molecular weight ladder standard used for SDS-polyacylamide gel electrophoresis (SDS-PAGE) was PAGE Ruler Plus Prestained Protein Ladder™. Fermentas™ supplied both standards.

2.3 Construction of plasmids constructs

A list of all the plasmids constructed can be found in Table 2.4.

TABLE 2.4: Plasmids used in this study

Name	Selectable markers, and Genes	Derivation of
pET11dHisA587T	Amp^r, $His_6Hsp82p^{A587T}$	pET11dHis
pET11dHisE381K	Amp^r, $His_6Hsp82p^{E381K}$	pET11dHis
pET11dHisG313S	Amp^r, $His_6Hsp82p^{G313S}$	pET11dHis

pET11dHisHsp82	Amp^r, His_6Hsp82p	pET11dHis
pET11dHisAha1	Amp^r, His_6Aha1p	pET11dHis
pET11dHisHch1	Amp^r, His_6Hch1p	pET11dHis
pET11dHisSba1	Amp^r, His_6Sba1p	pET11dHis
pET11dHisSti1	Amp^r, His_6Sti1p	pET11dHis

2.3.1 Construction of His_6-tagged Hsp82 mutants, and wild-type

The pET11dHis plasmid (Stratagene) was used for the construction of the wild-type Hsp82p, the Hsp82p mutants and co-chaperones [2]. The cassette of the $Hsp82^{A587T}$ mutant was obtained by PCR amplification using yeast genomic DNA as a template. A forward primer containing an Nde1 restriction site upstream of the ATG start codon, and reverse primer containing a BamH1 restriction site downstream of the TAA stop codon was used to amplify the $Hsp82^{A587T}$ cassette. The primers used for the amplification can be found in Table 2.5.

After PCR amplification the DNA cassette was resolved by electrophoresis using a 0.8-1.2% agarose gel that was infused with SYBR® Safe DNA Gel Stain (Invitrogen). This was to separate the DNA cassette from the PCR reagents, enzymes, and primers. After the DNA was resolved from these components, the bands were visualized using blue-light transilluminator ($\lambda \approx$ 450-495 nm) to confirm that the DNA was approximately the correct size, and excised. The DNA was purified from the agarose gel using QIAquick Gel Extraction kit (QIAGEN).

To prevent DNA contamination from this point on, only sterile pipette tips and microcentrifuge tubes were used. The purified Hsp82^{A587T} cassette and pET11dHis vector were digested with Nde1 and BamH1 restriction enzymes and buffers at 37°C for 15-30 minutes in a sterile 1.5 mL microcentrifuge. After digestion the purified Hsp82^{A587T} cassette and pET11dHis vector was resolved by electrophoresis using a 0.8-1.2% agarose gel that was infused with SYBR® Safe DNA Gel Stain (Invitrogen). This was to separate the DNA from the digestive enzymes, and confirm that the DNA had been digested using the approximate size of the insert or vector. The DNA was purified from the agarose gel using QIAquick Gel Extraction kit (QIAGEN).

Using the Nde1/BamH1 sticky end sites the Hsp82^{A587T} cassette was inserted into the multiple cloning site of a pET11dHis plasmid containing an ampicillin resistant marker (Amp^{r})[2]. The digested cassette and vector were ligated at room temperature overnight in a 2:1 molar ratio using the T4 DNA ligase and buffer following manufacturer's specification or instructions (Invitrogen or NEB).

The next day, the ligation reaction was used to transform competent *Escherichia coli* (*E. coli*) DH5-α cells using heat shock. Generally, 10% of a ligation reaction or approximately 0.25 µg of DNA was added to 50-100 µL of competent DH5-α cells in a 1.5 mL microcentrifuge tube. The mixture was then incubated on ice for 30 minutes, and subsequently subjected to a heat shock for 30-45 seconds in a water bath set to 42°C. This heat shock changed the fluidity of the E. coli membrane, allowing for our plasmid DNA that was successfully

ligated to enter the cells. Because the integrity of cells membranes is compromised, care should be taken not to agitate the cell when returning the microcentrifuge tube from the water bath to an ice bucket. The cells are placed on ice for 2 minutes, the cold temperatures are believed to stabilize the cell membrane, and reduce the thermal motion of the plasmid, so that it promoted the exogenous DNA to enter the cells [79]. 500-750 µL of Luria Broth (LB) was added to the cell mixture and the cells were incubated at 37°C for 30 minutes in order to repair their cell membrane damaged by the heat shock. After the cells had sufficient time to repair the damage done by the heat shock, the cells pelleted down by centrifuged at 14,000 rpm using a Eppendorf Centrifuge 5417 C/R for 20 seconds. After centrifugation of the cells, the supernatant was gently poured out, and the cell pellet resuspended with the 50-100 µL of LB remaining. The resuspended cells were then plated onto an LB agar plate containing 0.1 mg/mL ampicillin as a selective marker and incubated at 37°C overnight.

DH5-α cells that had been successfully transformed with the plasmid containing the Amp^r marker will reproduce to form colonies. Each colony selected was used to inoculate 5 mL of LB containing 0.1 mg/mL ampicillin, this is grown overnight at 37°C with agitation.

This mixture of cells and glycerol would be mix thoroughly kept at room temperature for about 1 hour before being transferred to a -80°C freezer to be stored for use in the future. The plasmid DNA was then isolated from the transformed DH5-α cells using a QIAprep Miniprep Kit (Qiagen) according to the manufacture's instruction. The plasmid was eluted in 30-50 µL of water and

quantified using a spectrophotometer at an absorbance of 260 nm (Thermo Scientific, NanoDrop). The sequences of the final plasmid were then confirmed by automated DNA sequencing performed by TAGC (University of Alberta, Department of Medical Genetics). Primers used in the sequencing reaction can be found in Table 2.5.

The other point mutations ($Hsp82^{E313K}$ and $Hsp82^{G313S}$) and the wild-type Hsp82 were obtained using QuikChange™ Site-Directed (Stratagene) mutagenesis on the $Hsp82^{A587T}$ cassette. Similar protocols were used in the purification, transformation, and sequencing of the DNA as the one listed above.

TABLE 2.5: Oligonucleotides used in this study

Oligonucleotides used in this study were ordered from International DNA technologies.

Name	**Sequence (5′ → 3′)**	**Application**
Hsp82 forward	GAG AGA CAT ATG GCT GGT GAA ACT TTT G	PCR amplification of DNA cassette
Hsp82 reverse	GAG AGA GGA TCC TCA CTA ATC TAC CTC TTC CAT TTC GGT G	PCR amplification of DNA cassette
Hch1 forward	GAG AGA CAT ATG GTT GTC TTG AAT CC	PCR amplification of DNA cassette
Hch1 reverse	GAG AGA GGA TTC TCA CTA AAC TTG TAT ATC CTT GAG TG	PCR amplification of DNA cassette
Aha1 forward	GAG AGA CAT ATG GTC GTG AAT AAC CCA AAT AAC TGG C	PCR amplification of DNA cassette
Aha1 reverse	GAG AGA GGA TCC TCA CTA TTA TAC GGC ACC AAA GCC G	PCR amplification of DNA cassette
Sba1 forward	GAG AGA CAT ATC TCA AAA GCT GTC GGT ATT G	PCR amplification of DNA cassette
Sba1 reverse	GAG AGA GGA TCC CTC ACT AAT CAA CTT CTT CAA CGG	PCR amplification of DNA cassette

Sti1 forward	GAG AGA CAT ATG GTT AAA GAA ACT AAG TTT TAC G	PCR amplification of DNA cassette
Sti11 reverse	GAG AGA GGA TCC TCA CTA TTG AGA TGC ACA TTG AAC	PCR amplification of DNA cassette

2.3.2 Construction of His_6-tagged co-chaperones

In this study we used four different co-chaperones: Aha1, Hch1, Sti1, and Sba1. The co-chaperone genes were ordered with the appropriate His_6-tag at the N-terminus from OpenBio Systems. Once I received the genes similar techniques of PCR amplification, DNA purification, digestion, ligation, transformation, and sequencing were utilized to the ones described in the construction of the pET11dHisHsp82^{A587T}. Primers used in PCR and sequencing reactions can be found in Table 2.5.

It should be noted that glycerol stocks was made of each co-chaperone and stored in the - 80°C freezer to be used in the future.

2.4 Isolation of large quantities of DNA from transformed *E.coli* (strain DH5α)

When larger quantities of plasmid DNA was needed, a 50 mL flask of LB containing 0.1 mg/mL ampicillin was inoculated with the glycerol stock of transformed DH5α *E.coli* containing the correct plasmid. The inoculated cultures were grown overnight at 37°C with agitation. The plasmid DNA was isolated QIAprep Midiprep Kit (Qiagen) using manufacturer's instruction. The plasmid DNA was eluted in 200-300 µL of water and quantified using spectrophotometer at an absorbance of 260 nm.

2.5 Expression of the protein in *E. coli* strains

2.5.1 Transformation of *E.coli* (strain BL-21DE3) with purified expression constructs by heat shock.

To optimize the expression of our proteins instead of purifying protein from *E. coli* from DH5α cells, the *E. coli* BL-21DE3 strain was used. The DNA had been purified from DH5-α cells expressing the appropriate plasmid using a Qiagen mini or midi-prep protocols This DNA was then used to transform the BL-21DE3 strain employing the same principles/protocols as the heat shock method in Section 2.3.1.

Depending on the concentration of DNA 0.25 - 2 µL of the correct purified plasmid construct were added to 50-100 µL of competent BL-21DE3 cells. The mixture was then incubated on ice for 30 minutes, and subsequently subjected to heat shock at 42°C for 30-45 seconds, and returned to ice for 2 minutes. 500-750 µL of LB was added to the cells, and the cells were incubated at 37°C for 30 minutes. Unlike the DH5-α cells transformation, instead of plating all the bacteria only 5-10% of the bacteria were plated. The reason for this being is that the DNA used for the transformation with BL-21DE3 were purified from DH5-α cells that have expressed the plasmid so I was not as concerned about the concentration of ligated DNA. After the cells were plated onto LB agar plate containing 0.1 mg/mL ampicillin, the plate was incubate at 37°C overnight.

2.5.2 Expression of yeast protein from *E. coli* strain BL-21DE3

Initially expression of the protein was done on a small scale to confirm that the clones picked from the transformation. Each colony selected from the LB

plate containing the transformed BL-21 cells were selected and used to inoculate 5 mL of LB media containing 0.1 mg/mL ampicillin. This culture was grown overnight at 37°C with agitation. A 500 µL sample was the taken of the starter culture and mixed with 500 µL of 30% glycerol. This mixture of cells and glycerol would be mix thoroughly kept at room temperature for about an hour before being transferred to a -80°C freezer to be stored for use in the future.

The starter culture was then used to inoculate a 50 mL flask of LB media containing 0.1 mg/mL ampicillin and grown for about 5 hours at 37°C or until OD_{600} in a range of 0.6-0.8. The cells were then induced for 6-12 hours with isopropyl-beta-thiogalactopyranoside (IPTG) to promote protein synthesis. Pre and post-induction samples were taken. The pre and post-induction samples were then resolved on a 10% sodium dodecyl sulfate polyacrylamide (SDS-PAGE) gel (with a 4% stacking gel) to confirm that there was induction of the protein expressed from the plasmid was approximately the correct molecular weight.

After the Bl-21 cells were confirmed to be suitable for expression, inoculate 25 mL culture(s) of LB media containing 0.1 mg/mL ampicillin. The culture(s) were grown at 37°C with agitation overnight. Each 25 mL culture was used to inoculate a 750 mL culture of LB media containing 0.1 mg/mL ampicillin. The culture was grown to an OD_{600} of 0.6-1.8 where indicated and a 20 µL sample was taken (pre-induction sample) before the culture was induced overnight at 37°C with IPTG. The next day a 20 µL post induction sample was taken before cells were harvested. The pre-and post induction samples were

resolved on a 10% SDS-PAGE gel (with a 4% stacking gel) before the lysis and purification steps to confirm that the culture expressed the protein of interest.

To harvest the cells a Beckman Coulter Avanti J-25 centrifuge was used with a JLA 10, 500 rotor to spin the cultures at 8000-10000 rpm for 15-20 minutes. The cells were then resuspended in 1x PBS, and transferred to a 50 mL falcon tube. The cell mixture was then pelleted using a Thermo Scientific Sorvall Legend T + with a multiple carrier swinging bucket 7500 6445 rotor that was at 4150 rpm for 20-30 minutes. The supernatant was poured out and at this point the cells can be stores at 80°C for future purifications or we can start the first steps of purification.

2.6 Purification of Expressed Protein

All of our purifications were performed using an ÄKATA FPLC system with a Frac-950 fraction collector. To purify our proteins I combined two different chromatography techniques: immobilized metal ion adsorption chromatography (IMAC), and gel filtration chromatography (GF). I had tried other chromatography techniques such as, ion exchange chromatography (IEX), or hydrophobic interaction chromatography (HIC) but did not find that these procedures improved the purification of the proteins. These steps were later eliminated from the purification procedure. Below was a generalization of the methods used to purify our proteins.

2.6.1 Harvest and lysis of cells

Cells were harvested by centrifugation, the cells where then either placed in the -80ºC or resuspended in 50-75 mL of IMAC A, or resuspension buffer (Table 2.6).

After the cells had been resuspended in IMAC A or resuspension buffer an EDTA-free protease inhibitor tablet or HALT protease inhibitor liquid was added. Cells were lysed using an emulsiflex As lysis occurs the consistency of the cell suspension should change to become more viscous and opaque.

The proteins was then separated from cell debris, and unlysed cells by ultracentrifugation in a Beckman Coulter Optima L-100K using a Ti60 rotor. The lysed cells were spun at 36,000 rpm for 30 minutes. The resultant lysate should be clear and there should large pellet of cell debirs and insoluble protein with a glassy looking lipid ring at the bottom of the tube. As much of the lysate was removed above the pellet without disturbing it and placed in a falcon tube. This supernatant was used in later purification steps.

2.6.2 Immobilized metal ion adsorption chromatography (IMAC)

The first step was used for all of our protein purifications was immobilized metal ion chromatography. A 5 mL HisTrap HP column GE Healthcare Life Science) was used for the IMAC purification. The buffers used in the initial purification are detailed in Table 2.6. The initial the protocol we used for an IMAC purification is outlined in Table 2.7. The last wash step ensured that all the protein (particularly our protein) was competed off the column. For many of the proteins I purified, I found that there was poor resolution between the 2% and 5%

step. This became a problem when our column became saturated and some of the desired protein was found in the 5% wash. To increase our resolution we later modified the protocol by suspending the cells in resupension buffer, which contained 20 mM Imdiazole. The IMAC protocol was modified to omit the 2% IMAC wash step, any protein that was eluted the previous 2% step would now be found in the flow through (Table 2.8). We monitor protein that was eluted off the column using the protein absorption of light at the 280nm (A_{280}). Elution samples corresponding to high levels of A_{280} absorption on the chromatogram of the purification were resolved on an 10% SDS-PAGE gel, and factions were pooled accordingly.

TABLE 2.6: List of chromatography buffers

Buffer	Composition
IMAC A	25 mM sodium phosphate pH 7.2, 500 mM sodium chloride, 1 mM magnesium chloride , 5 mM β-Mercaptoethanol
IMAC B	25 mM Hepes pH 7.2, 500 mM sodium chloride, 1 mM magnesium chloride, 1 M imidazole, 5 mM β-Mercaptoethanol
Resuspension IMAC Buffer	25 mM Sodium Phosphate pH 7.2, 500 mM Sodium Chloride, 1 mM Magnesium Chloride, 20 mM Imidazole, 5 mM β-Mercaptoethanol
Chaperone gel filtration buffer	25 mM Hepes pH 7.2, 10 nM sodium chloride
Co-chaperone gel filtration buffer	25 mM Hepes pH 7.2, 50 nM sodium chloride

TABLE 2.7: Schematic of Protocol 1 of a typical IMAC purification used

Step	Procedure
Sample injection	50-175 mL injection; 0.2-0.5 mL/min flow rate
Step gradient 1 wash	2% IMAC B for 10-25 mL column volumes
Step gradient 2 wash	5% IMAC B for 10-25 mL column volumes
Linear gradient elution	5% to 100% IMAC B over 20-50 mL
Step gradient 3 wash	100% IMAC B over 10 column volumes
Fraction collection	1 mL fractions

TABLE 2.8: Schematic of Protocol 2 a typical IMAC purification used when sample was resuspended with 20 mM Imdiazole

Step	Procedure
Sample injection	50-175 mL injection; 0.2-0.5 mL/min flow rate
Step Gradient 1	5% IMAC B for 10-25 mL column volumes
Linear gradient	5% to 100% IMAC B over 20-50 mL
Step gradient 3 wash	100% IMAC B over 10 column volumes
Fraction collection	1 mL fractions

2.6.3 Gel filtration chromatography (GF)

This was the final step in the purification of all of our proteins was gel filtration chromatography. After the appropriate fractions were pooled from the IMAC purification, generally the protein was relatively pure (85-100%). The pooled fractions were then concentrated to 250-500 µL using an Amicon Ultra Centrifugal Filter Device For Hsp82p and mutants proteins I used a 10,500 MWCO, while for the co-chaperones I used a 3,000 MWCO. The protocol for a gel filtration was the same for all the proteins used in this study and can be found in Table 2.9. For Hsp82p and mutants proteins we used a Superose 6 Gel filtration column (GE Healthcare Life Science), for the co-chaperones we used a Superdex 75 Gel filtration column (GE Healthcare Life Science).

TABLE 2.9: Schematic of a typical gel GF purification

Step	Procedure
Sample injection	250-500 µL sample loaded into a manual loop
Linear gradient	1% to 100% gel filtration buffer over 1 column volume
Fraction collection	0.5 mL fractions

2.7 ATPase experiments

After the protein had been purified, I used the protein to study the ATPase activity of the wild-type Hsp82p, and the Hsp82p mutants. I measured the ATPase activity of the wild-type Hsp82p, and the Hsp82p mutants using an indirect enzyme-coupled assay (Figure 2.1). Hsp82 hydrolyzes the ATP to form ADP; this ADP is phosphorylated by pyruvate kinase (PK) during the conversion of phosphoenolpyruvate (PEP) to pyruvate. Pyruvate is then converted to lactate by lactate dehydrogenase (LDH). This second reaction of the conversion of pyruvate to lactate requires the oxidation of one molecule of NADH to form NAD^+. Both NADH and NAD^+ have distinct UV absorption properties; NADH absorbs UV light at 340 nm, while NAD^+ absorbs UV light at 260 nm. The decrease in absorption of UV light at 340nm over time monitors the conversion of NADH to NAD+. The rate of NADH depletion can be used to calculate ATP hydrolysis, as both are consumed stoichiometrically in a 1:1 ratio in this two-step reaction.

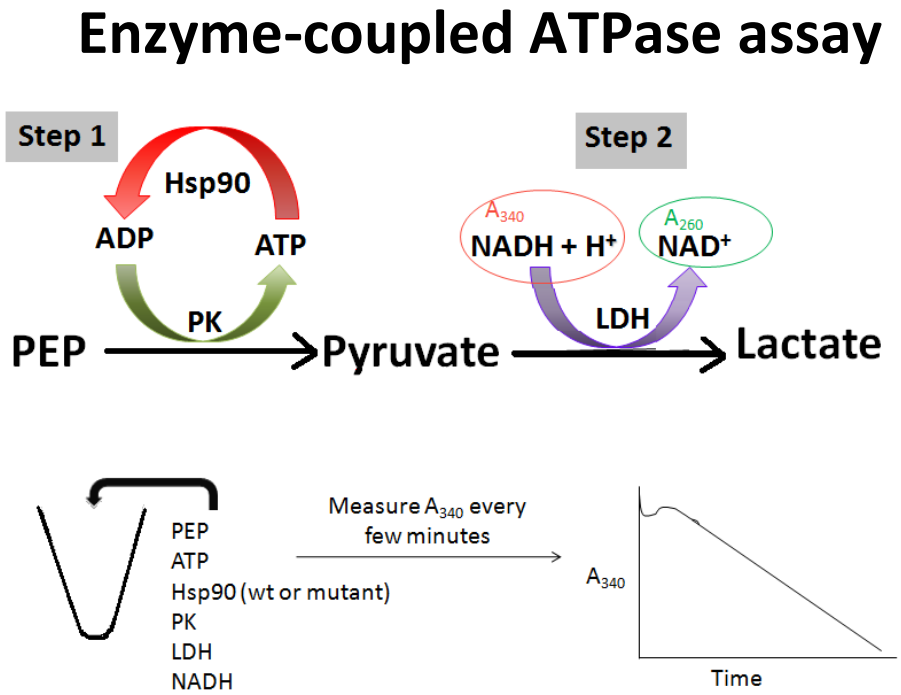

FIGURE 2.1: Schematic diagram for the enzyme-coupled ATPase assay

A enzyme-coupled ATPase assay is based the two step conversion of phosphoenolpyruvate (PEP) to lactate. Within the assay we have Hsp82p or Hsp82 mutant hydrolyzes ATP, this reaction is coupled with the conversion of PEP to pyruvate by the enzyme pyruvate kinase (PK) (Step 1). PK is able to regenerate ATP by phosphorylating the ADP by product of Hsp90 ATPase activity. Pyruvate is then converted to lactate by the enzyme lactate dehydrogenase (LDH) (Step 2). Step 2 requires the oxidation of NADH to NAD^+. We measured the decrease in absorption at 340nm correlates with the decrease in NADH. As both NADH and ATP are consumed stoichiometrically in a 1:1 ratio using the OD_{340nm} we can measure the rate of ATP hydrolysis of Hsp82p or mutants.

Chapter 3

Biochemical Characterization of the ATPase activity of three Hsp82 point mutants: Hsp82p^{A587T}, Hsp82p^{G313S}, and Hsp82p^{E381K}

3.1 Overview

This chapter focuses on the characterization of the ATPase activity of three point mutants of Hsp82p: Hsp82p^{E381K}, Hsp82p^{A587T}, and Hsp82p^{G313S}. ATP hydrolysis by Hsp82p occurs near the end of the chaperone cycle; because of this we are able to use the ATPase activity as a reporter for the ability of individual Hsp82p mutants to progress through the cycle. The goal in characterizing the ATPase activity of each mutant is to discover how these mutants are defective in the Hsp90 cycle, and distinguish a function for the co-chaperone Hch1.

Data from our lab has shown that yeast expressing Hsp82p^{E381K}, Hsp82p^{A587T}, and Hsp82p^{G313S} display temperature sensitive phenotypes, and become inviable at high temperatures. Interestingly, the ability of these three Hsp82p mutants to function is differentially influenced by the co-chaperone, Hch1p. Our lab has demonstrated that overexpression of *HCH1* rescues the temperature sensitive phenotype of yeast expressing Hsp82p^{E381K} (Figure 1.9). Conversely, the temperature sensitive phenotypes of yeast expressing Hsp82p^{A587T} or Hsp82p^{G313S} were suppressed by the deletion of *HCH1* (Figure 1.10). From these observations I had hypothesized that the defect of Hsp82p^{E381K} is rescued by the presence of Hch1p, while the molecular defect of both Hsp82p^{A587T} and Hsp82p^{G313S} is exacerbated by the presence of Hch1p.

Before I could study the effect that Hch1p has on the mutants, I needed to characterize the ATPase activity of the Hsp82p^{E381K}, Hsp82p^{A587T} and Hsp82p^{G313S} mutants. In addition to characterizing the intrinsic ATPase rate of the mutants, I also studied the effect of three other co-chaperones, Aha1p, Sti1p, and

Sba1p, which are known to influence the ATPase activity of Hsp82p. By studying the ATPase activity of the three mutants with these co-chaperones, I hope to learn more about the unique molecular defect of each mutant. After determining at which step(s) of the Hsp90 cycle that Hsp82p^{E381K} was defective, I can examine if the presence of Hch1p rescues Hsp82p^{E381K} at the defective step(s). I will also characterize both Hsp82p^{A587T} and Hsp82p^{G313S} using the same co-chaperones to find at which step either mutant is similar to the wild-type, and observe if the presence of Hch1p negatively affects the mutants' ability to function at certain steps.

All of the proteins used in the assays were purified using similar protocols. Each protein was expressed with a His_6- tagged, and in first step I used a nickel resin to purify the protein. The IMAC protocol and buffers are outlined in Table 2.7and Table 2.8. The final purification step for all of our proteins was a gel filtration. To purify Hsp82p and the mutants, I used a Superose 6 column, while for the co-chaperones I used a Superdex 75 column. The gel filtration buffers used for the chaperone, mutants, and co-chaperones are as outlined in Table 2.9.

3.2 Measurement of the intrinsic and Aha1p-stimulated ATPase rate of wild-type Hsp82p, and the Hsp82p^{E381K}, Hsp82p^{A587T}, and Hsp82p^{G313S} mutants

ATP hydrolysis by Hsp82p occurs when the N-terminal domains of each monomer dimerizes to form a 'closed' conformation. This closed conformation is rarely acquired by the highly dynamic Hsp90 dimer in the absence of co-chaperones that influence this structural transition. I tested the wild-type, Hsp82p^{E381K}, Hsp82p^{A587T}, and Hsp82p^{G313S} mutants' intrinsic ATPase activity

(Figure 3.1). What I found was that the wild-type and Hsp82p^{E381K} mutant had comparable intrinsic rates (Figure 3.1 A), while both the Hsp82p^{A587T} and Hsp82p^{G313S} mutants have lower intrinsic rates than the wild-type (Figure 3.1B and Figure 3.1C).

The co-chaperone, Aha1p binds to the closed conformation of Hsp82p and robustly stimulates the ATPase rate. In order for Aha1p to stimulate the ATPase activity of Hsp82, Aha1p must interact with the dimer at two discrete sites; the Aha1p N-terminal domain interacts with the middle domain of Hsp82p, and the Aha1p C-terminal domain interacts with the N terminal domain of Hsp82p [32,73]. We found that all of the mutants were able to be stimulated by Aha1p (Figure 3.1). Under similar conditions with each mutant, the Aha1p stimulation is evident with the increase in activity seen when comparing the third column, with the fourth column in each assay (Figure 3.1). Of the three mutants only Hsp82p^{A587T} was robustly stimulated by Aha1p (Figure 3.1B). A closer look at the Hsp82p^{A587T} experiment in Figure 3.2 shows the effect of Aha1p on Hsp82p^{A587T} ATPase activity was much greater than on the wild-type. When stimulated rates of both the wild-type Hsp82p and Hsp82p^{A587T} are compared, we found that Hsp82p is stimulated 4.7 fold, while under the same conditions Hsp82p^{A587T} was stimulated by 18.5 fold (Figure 3.1B).

Under similar conditions, the Hsp82p^{E381K} and Hsp82p^{G313S} mutants have lower stimulated ATPase rates when compared to the wild-type (Figure 3.1A and and (Figure 3.1C). The lower Aha1p stimulated rates seen in Hsp82p^{E381K} and Hsp82p^{G313S} be due to a variety of reasons such as the inability to bind to ATP,

Aha1p, or a mechanical problem in its ability to hydrolyze ATP. To address the possibility that inability of Hsp82p^{G313S} to be fully be stimulated by Aha1p could be due to the impaired ability to bind and hydrolyze ATP, an ATPase assay was done where ATP concentration varied in Aha1p stimulated reactions. For each variant of Hsp82p we expected there to be a point of saturation. This point would be the concentration of ATP where the maximal ATPase rate is reached and cannot be increased by the addition of more ATP. The published affinity of the N-terminus of Hsp82 for ATP is about 132 μM [80]. We used a range of concentrations from 0.1 mM - 4 mM of ATP. The lowest ATP concentration used (0.1 mM) is close to the publish affinity of Hsp82p for ATP, while the highest concentration (4 mM) is about 30 times the published affinity. Each Hsp82p variant was plotted as a percentage of the ATPase rate at 4 mM, assuming that at this concentration the maximum ATPase rate (V_{max}) is achieved. What I found was that the concentration required for Hsp82p^{G313S} to reach the half of the maximal rate (K_m) is about 0.1 mM ATP, while the K_m for both Hsp82p^{A587T} and Hsp82 was less than 0.1 mM ATP (Figure 3.2).

Next we addressed whether the defect in Hsp82p^{G313S} is a result of a reduced affinity or an inability to bind to Aha1p. To address the question I did an ATPase experiment where each Hsp82 variant was stimulated with varying concentrations of Aha1p. By changing the concentration of Aha1p present in each reaction, I can determine if there is a difference in the Aha1p needed for each mutant to reach maximal stimulation. The data was plotted as a fold increase of the wild-type intrinsic ATPase rate. Figure 3.3 shows that Aha1 does not

stimulate Hsp82p^{G313S} to the extent as seen with Hsp82p^{A587T} or Hsp82p. Even at a concentration of 16 μM of Aha1p, Hsp82p^{G313S} is only stimulated about 8 fold from the intrinsic wild-type ATPase levels. But the data with Hsp82p^{G313S} mutant was inconclusive as the signal to noise ratio was very low. At the same concentration of Aha1, Hsp82p^{A587T} and wild-type Hsp82p is stimulated by 18 and 19 fold, respectively.

3.3 Measurement of Sti1p-inhibited ATPase rate of the wild-type Hsp82p, and the Hsp82p^{E381K}, Hsp82p^{A587T}, and Hsp82p^{G313S} mutants

After characterizing the three Hsp82p mutants in terms of their intrinsic and stimulated rate, I next wanted to characterize the three mutants in regards to another co-chaperone Sti1p. Sti1p has the opposite effect that Aha1p does on Hsp82; inhibiting the ATPase rate by preventing N-terminal dimerization [29,56]. Using our enzyme-linked assay I was able to measure the effects of Sti1p on the wildtype Hsp82, and Hsp82pE381K, Hsp82p^{A587T}, and Hsp82p^{G313S} mutants in an Aha1p stimulated reaction. What I found was that Sti1p was able to inhibit the simulated ATPase activity of Hsp82p^{A587T} similarly to wild-type (Figure 3.4). It appeared that Sti1p had the same affect on Hsp82p^{G313S}, but the signal to noise ratio with Hsp82p^{G313S} was too low to conclusively state that Sti1p was able to inhibit the ATPase activity of Hsp82p^{G313S} mutant (Figure 3.4). Interestingly, under the same conditions, the Hsp82p^{E381K} mutant was not inhibited by Sti1p (Figure 3.4).

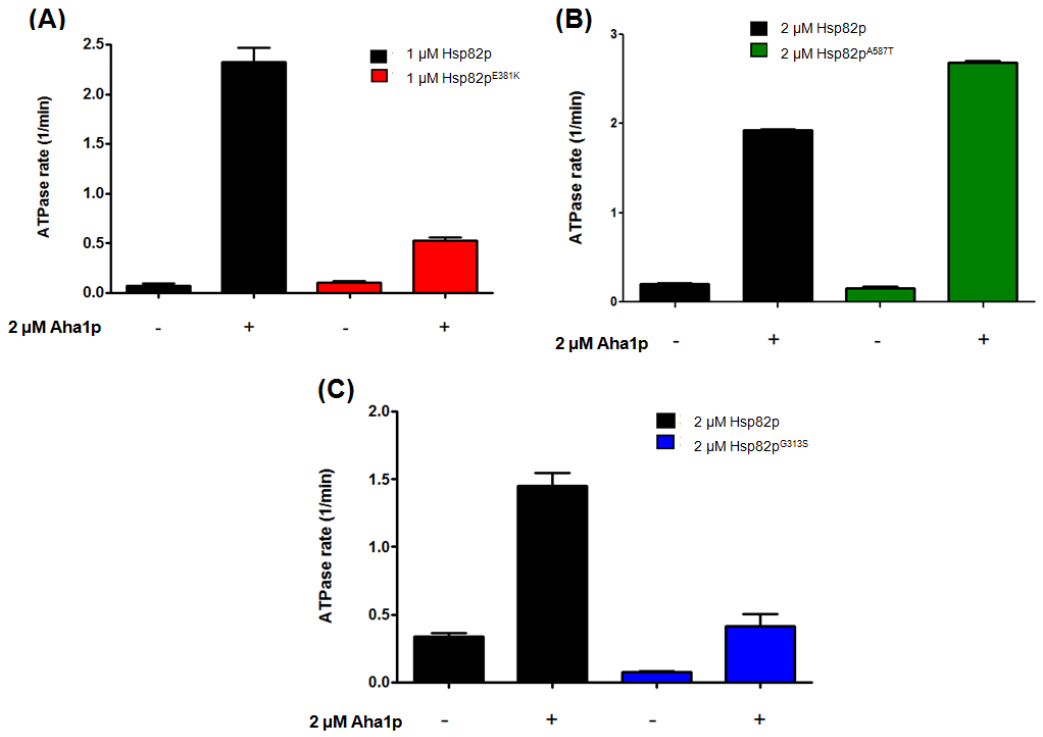

FIGURE 3.1: The effect of Aha1p on the ATPase activity of Hsp82p, Hsp82p^{E381K}, Hsp82p^{A587T}, and Hsp82p^{G313S}

(A) A typical ATPase experiment was conducted on Hsp82p [81] and Hsp82 p ^{E381K} (red). 1 µM of Hsp82p or Hsp82p^{E381K} was used. The ATPase rate was measured at a permissive temperature (30°C) in the absence or presence of 2 µM Aha1p.

(B) A typical ATPase was conducted on Hsp82p [81] and Hsp82p^{A587T} (red). 2 µM of Hsp82p or Hsp82p^{A587T} were used. The ATPase rate was measured at a permissive temperature (30°C) in the absence or presence of 2 µM Aha1p.

(C) A typical ATPase was conducted on Hsp82p [81] Hsp82p^{G313S} (blue). 2 µM of Hsp82p or Hsp82p^{G313S} was used. The ATPase rate was measured at a permissive temperature (30°C) in the absence or presence of 2 µM Aha1p.

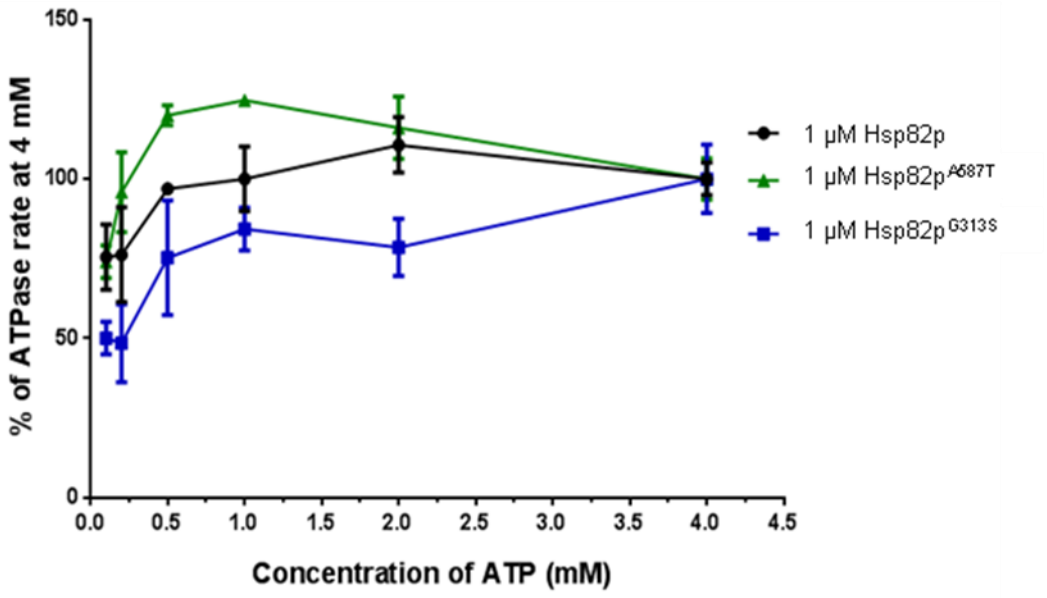

FIGURE 3.2: Effect of increasing concentrations of ATP on the ATPase activity of Hsp82p, Hsp82p^{A587T}, and Hsp82p^{G313S}

A representative ATPase experiment was conducted with Hsp82p [81], Hsp82p^{A587T} (green), and Hsp82p^{G313S} (blue) in the presence of 2 µM Aha1p with increasing concentrations of ATP. 1 µM of Hsp82p, Hsp82p^{A587T}, or Hsp82p^{G313S} was used. The data of each individual Hsp82p variant was plotted as a percentage of the ATPase activity at 4 mM. The concentrations of ATP tested were: 0.1 mM, 0.2 mM, 0.5 mM, 1 mM, 2 mM, and 4 mM. This experiment was conducted at a permissive temperature of 30°C.

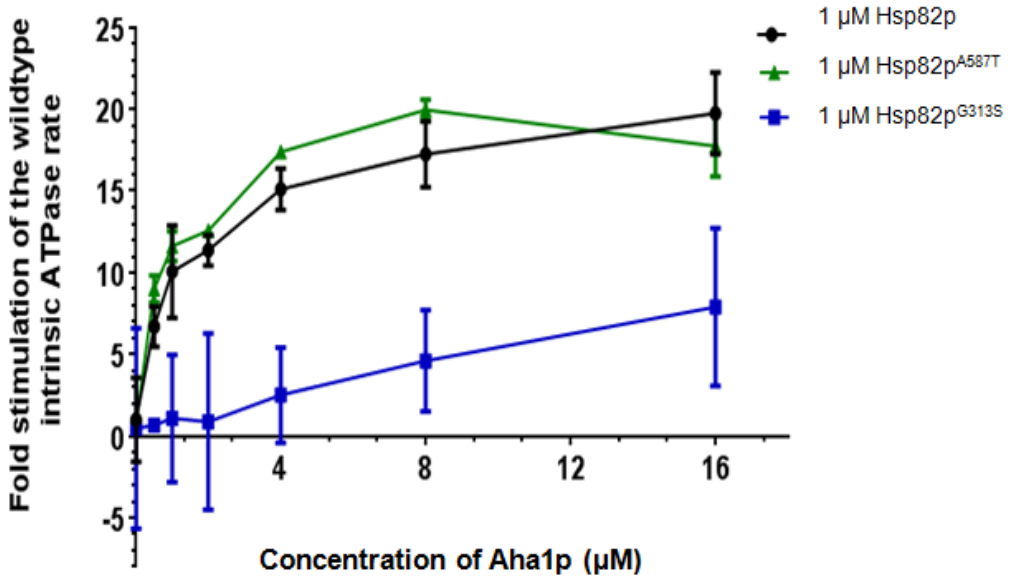

FIGURE 3.3: Effect of increasing concentrations of Aha1p on the ATPase activity of Hsp82p, Hsp82p^{A587T}, and Hsp82p^{G313S}

A representative ATPase experiment was conducted with Hsp82p [81], Hsp82p^{A587T} (green), and Hsp82p^{G313S} (blue). 1 μM of Hsp82p, Hsp82p^{A587T}, or Hsp82p^{G313S} was used. The data of each individual Hsp82p variant was plotted as fold stimulation of the wild-type intrinsic level. The concentrations of Aha1p tested were: 1 μM, 2 μM, 4 μM, 8 μM, and 16 μM. This experiment was conducted at a permissive temperature of 30°C.

3.4 Measurement of Sba1p-inhibited ATPase rate of wild-type Hsp82p, and the Hsp82p^{A587T}, and Hsp82p^{G313S} mutants

Another co-chaperone I wanted to characterize the mutants Hsp82p^{A587T} and Hsp82p^{G313S}, with was Sba1p. Sba1p is another co-chaperone that influences the ATPase activity of Hsp82p. Structural evidence has shown that Sba1p preferentially binds the ATP bound state of Hsp90, and inhibits the ATPase rate [68,82].

When Sba1p was added to an Aha1p-stimulated reaction with wild-type Hsp82p there was inhibition of the stimulated ATPase activity but not to the same extent as seen with Sti1p. The same pattern was seen for the Hsp82p^{A587T} mutant (Figure 3.6). Once again the signal to noise ratio with the Hsp82p^{G313S} mutant was too low to make any conclusion.

3.5 Investigating the effect of Hch1p on the intrinsic, and Aha1p-stimulated ATPase rate of wild-type Hsp82p, and the Hsp82p^{A587T}, and Hsp82p^{E381K} mutants

The focus of my study was to investigate a novel function for the co-chaperone Hch1p. From the yeast data in our lab, I had formulated a hypothesis that Hch1p rescued the defect of the Hsp82p^{E381K} mutant, while exacerbating the defect of Hsp82p^{A587T} and Hsp82p^{G313S} (Figure 1.9 and Figure 1.10). Before I could the novel function of Hch1p, I needed to characterize the three mutants terms of their intrinsic ATPase rate, and their relationship with Aha1p, Sti1 and Sba1p.

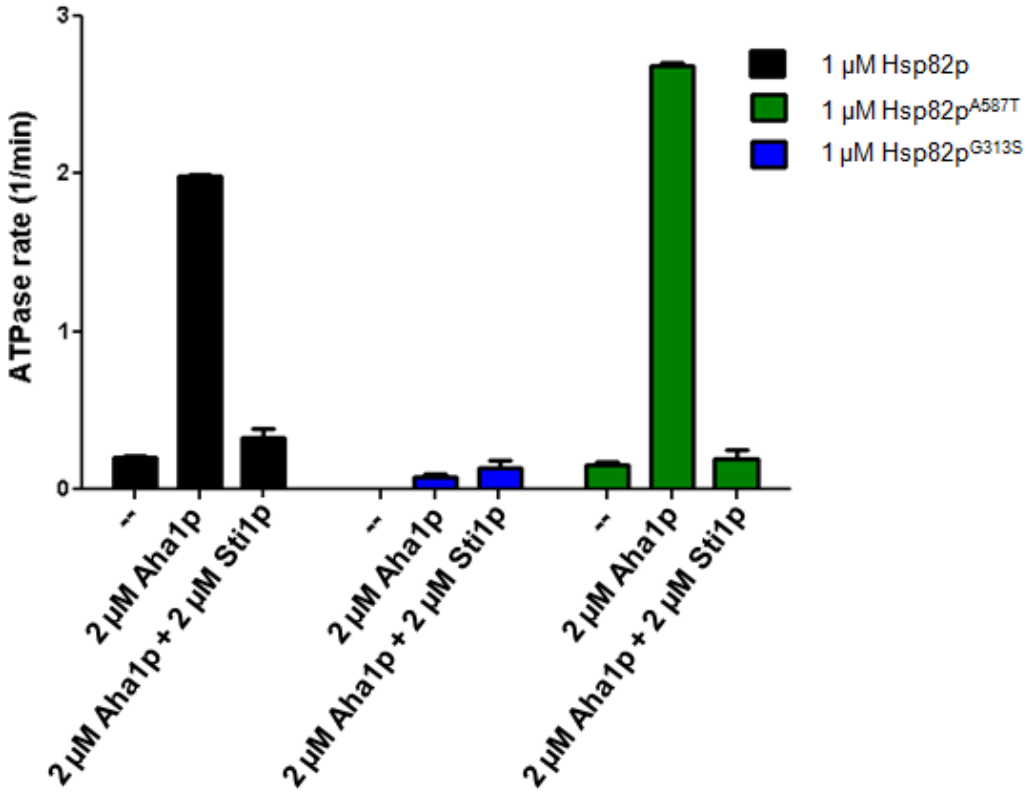

FIGURE 3.4: Effect of Sti1p on the stimulated ATPase activity of Hsp82p, Hsp82p^{A587T}, and Hsp82p^{G313S}

A representative ATPase experiment was conducted with Hsp82p [81], Hsp82p^{A587T} (green), and Hsp82p^{G313S} (blue). 1 μM of Hsp82p, Hsp82p^{A587T}, or Hsp82p^{G313S} was used. The ATPase rate was measured at a permissive temperature (30°C). Both the intrinsic and stimulated rate (2 μM Aha1p) of the Hsp82p, and Hsp82p^{A587T} was measured with or without 2 μM Sti1p.

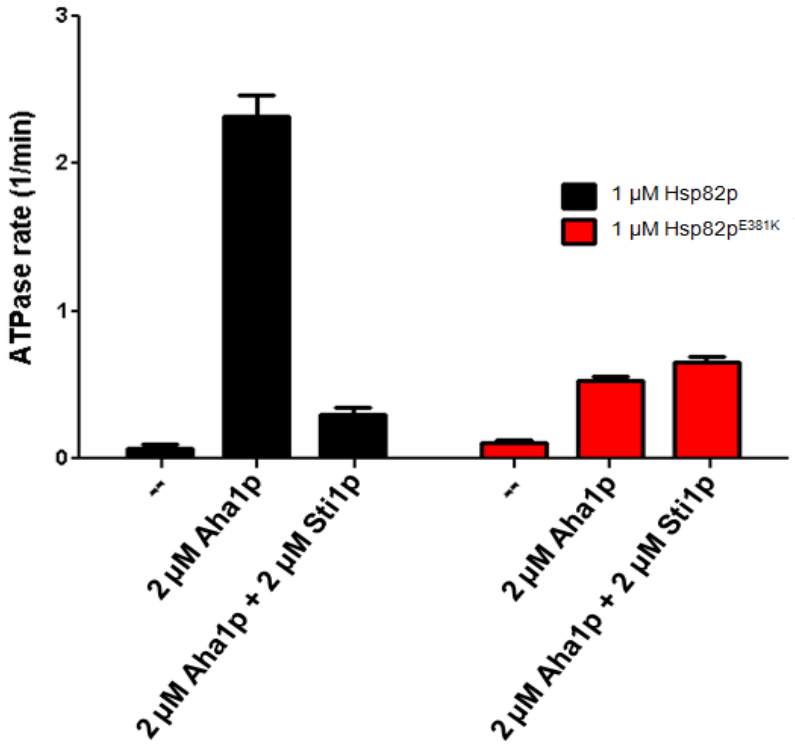

FIGURE 3.5: Effect of Sti1 on the stimulated ATPase activity of Hsp82p, and Hsp82p^{E381K}

A representative ATPase experiment was conducted with Hsp82p [81], Hsp82p^{E381K} (red). 1 µM of Hsp82p, or Hsp82p^{E381K} was used. The ATPase rate was measured at a permissive temperature (30°C). Both the intrinsic and stimulated rate (2 µM Aha1p) of the Hsp82p, and Hsp82p^{E381K} was measured with or without 3 µM Sti1p.

I wanted to discover at which step of the Hsp90 cycle the Hsp82p^{E381K} mutant was defective, and if the presence of Hch1p corrected this impairment. With Hsp82p^{A587T} and Hsp82p^{G313S} I was looking for the opposite relationship. I was looking at which steps did the mutants act similarly to wild-type, but the presence of Hch1p hindered the mutants ability to function properly.

In my characterization of the mutants I found that Hsp82p^{E381K} is defective at two steps in the Hsp90 cycle: Hsp82p^{E381K} is not robustly stimulated by Aha1p, and this low stimulated rate is not inhibitable by Sti1p (Figure 3.1A and Figure 3.5). With the Hsp82p^{A587T}, I found that the mutant had a slightly elevated Aha1p stimulated ATPase activity, when compared to the wild-type (Figure 3.1B). Also Hsp82p^{A587T} ability to be inhibited by either Sti1p, or Sba1p was similar to that of the wild-type (Figure 3.4, and 3.6). The last mutant I studied Hsp82p^{G313S}, was such a poor ATPase, and the signal to noise ratio in the assay was very low making it difficult to study, or form conclusions about the data I obtained (Figure 3.1C, Figure 3.2, and Figure 3.3). This made Hsp82p^{G313S} an unsuitable a candidate for my hypothesis – we have since learned that Hsp82p^{G313S} mutant is likely not completely defective at every step, but when we purify the mutant we remove a stabilizing interaction with another protein resulting in misfolded protein. For this reason for the characterization with Hch1p was only done with Hsp82p^{A587T}, and Hsp82p^{E381K}.

The first thing that I investigated was if the presence of Hch1p hindered Hsp82p^{A587T}, or if it improved Hsp82p^{E381K} ability to be stimulated by Aha1p. To

test this, an experiment was done where the mutants was tested with or without Hch1p and/or Aha1p. When I tested Hsp82p^{A587T} I found that Hch1p was able to weakly stimulate Hsp82p, similar to Aha1p (Figure 3.7). This confirms previous reports that the presence of Hch1p, at high concentrations is capable of increasing the ATPase activity but not to the same extent as Aha1p [32,70]. Because Hch1p and the N-terminus of Aha1p share similar structure it competitively binds to the same site on the middle domain of Hsp90, therefore I had predicted that by adding Hch1p to a stimulated Hsp82p^{A587T} or wild-type reaction, and there would be a decrease in ATPase activity due to competitive binding of the same site. Contrary to my hypothesis, I found was Hch1p enhanced the ATPase activity of Hsp90. As seen in column four and eight of Figure 3.7, there is an increase in ATPase rate when both Hch1p and Aha1p were added to Hsp82p^{A587T}, or the wild-type reaction. The presence of Hch1p did not hinder the ability for Aha1p to stimulate the mutant; this meant that this was not the step that Hch1p exacerbated in the Hsp82p^{A587T} cycle (Figure 3.7).

When the same experiment was done with Hsp82p^{E381K}, I was able to reproduce the weak stimulation by Hch1p with the wild-type Hsp82p (Figure 3.8). This stimulation of the ATPase activity due to Hch1p alone is not seen with Hsp82pE381K (Figure 3.8, column 7). Looking at Figure 3.8, when comparing the second and sixth column once again we see that the mutant Hsp82p^{E381K} was not stimulated by Aha1p to the same extent as the wild-type Hsp82p. Interestingly, we did find was that the addition of both Aha1p and Hch1p remarkably rescued Hsp82p^{E381K} inability to be stimulated (Figure 3.8 column

eight). When the second column is compared to the eighth column in Figure 3.8, we can see that there is an increase in ATPase activity, and Hsp82p^{E381K} activity is restored to wild-type levels. This finding that was very exciting for our lab, as it shows that Hch1p rescued the molecular defect of Hsp82p^{E381K}, and Hch1p is capable of influencing steps in the "late" stage of the Hsp90 cycle.

To confirm my findings, the experiment needed to be repeated for the last time, but more protein needed to be purified, particularly Hch1p. Hch1p has always been a protein that is difficult to purify. Much of the protein is insoluble. To try to overcome this issue a new vector of HisHch1p was made, transformed into new BL-21 *E. coli* cells, expressed and purified similarly to all of the other proteins I used in the study. Surprisingly, this new clone had less of a solubility issue. Protein was still lost during the ultracentrifugation step but with this new clone, but I was able to recover a significantly more protein then with the old clone.

When the ATPase assay was repeated, we saw similar results as the first experiment, when the wildtype or Hsp82p^{E381K} are present with Aha1p or newly purified Hch1p alone (Figure 3.9). When we added both Aha1p and new Hch1p there was no rescue of the ATPase activity of Hsp82p^{E381K} (Figure 3.9, column eight). If I were to compare the trends of the experiment conducted in Figure 3.8 and Figure 3.9, I would not see a difference in pattern with the exception of the last column in each experiment. This meant that the old Hch1 was somehow different from the new Hch1p.

The difference between the old and new preparations of the Hch1p protein had to be addressed before I could continue with the experiments. To confirm the results that I got from the different preparations, a small scale experiment was done to compare the old and the new Hch1p samples. Since we only had a very limited amount of the old Hch1p, the experiment was only done in duplicate and proper controls were not done. Because I was just looking at trends – specifically if the old Hch1p was able to rescue Hsp82p^{E381K}, while the new Hch1p was not I was not too concerned about creating a publishable figure. This experiment was intended to rule out that possible error such as contamination that could have occurred when the experiment was first conducted. The results confirmed that the old Hch1p still rescued the Hsp82p^{E381K}, while the new Hch1p did not.

The next steps I did was to try to determine how the two Hch1p preparations differed, and to find what was in the old preparation that causes the prominent rescue in the ATPase activity of the Hsp82p^{E381K} mutant. Both samples of purified Hch1p were resolved on an SDS-PAGE gel (Figure 3.10). This allowed me to look for contaminating proteins and roughly compare the sizes of the protein. As seen in the Figure 3.10, both samples looked identical on the gel in terms of size and purity.

Earlier on in my project I had experimented with different tags (His_6-tag, ThrHis_6-tag, and TEVHis_6-tag), to eliminate the possibility that I mixed the tags up I sequenced the plasmid with both the proteins were expressed from. The pET vector was first isolated from the BL-21 cells, re-transformed into DH-5α cells, and then expressed, purified, and sent for sequencing. At the same time, the

protein was also prepared for mass spectrometry. The mass spectrometry and sequencing data indicated that both proteins were His_6Hch1p.

Knowing that we have two samples of HisHch1 that affect our mutants differently all of our previous findings done with the old preparation of Hch1p needs to be re-evaluated. Unfortunately, I do not have enough of the old preparation to continue investigating the difference between the two Hch1p. The result that Hch1p does not rescue the defect of the $Hsp82p^{E381K}$ mutant has been reproduced and we have now accepted this to be true.

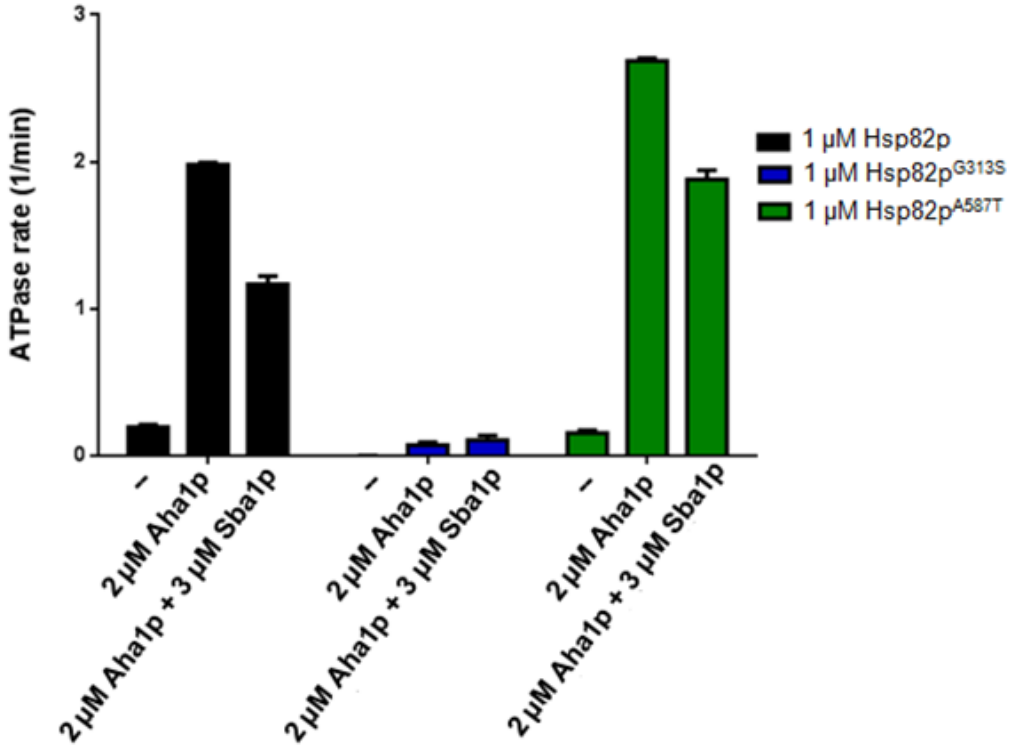

FIGURE 3.6: Effect of Sba1p on the stimulated ATPase activity of Hsp82p, Hsp82p^{A587T}, and Hsp82p^{G313S}

A representative ATPase experiment was conducted with Hsp82p [81], Hsp82p^{A587T} (green), and Hsp82p^{G313S} (blue). 2 µM of Hsp82p, Hsp82p^{A587T}, or Hsp82p^{G313S} was used. The ATPase rate was measured at a permissive temperature (30°C). Both the intrinsic and stimulated rate (2 µM Aha1p) of the Hsp82p, and Hsp82p^{A587T} was measured with or without 3 µM Sba1p.

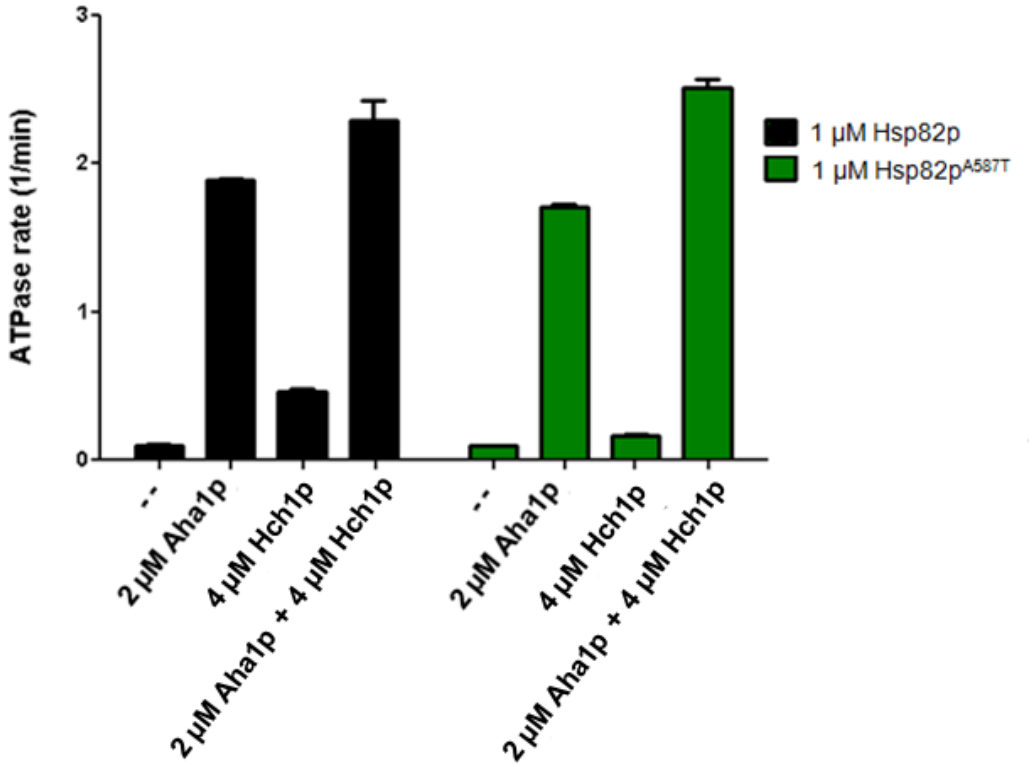

FIGURE 3.7: Effect of Hch1p on the stimulated and non stimulated rate of Hsp82p, and Hsp82p^{A587T}

A representative ATPase experiment was conducted with Hsp82p [81] and Hsp82p^{A587T} (green). 2 µM of Hsp82p, or Hsp82p^{A587T} was used. The ATPase rate was measured at a permissive temperature (30°C). Both the intrinsic and stimulated rate (2 µM Aha1p) of the Hsp82p, and Hsp82p^{A587T} was measured with or without 4 µM Hch1p.

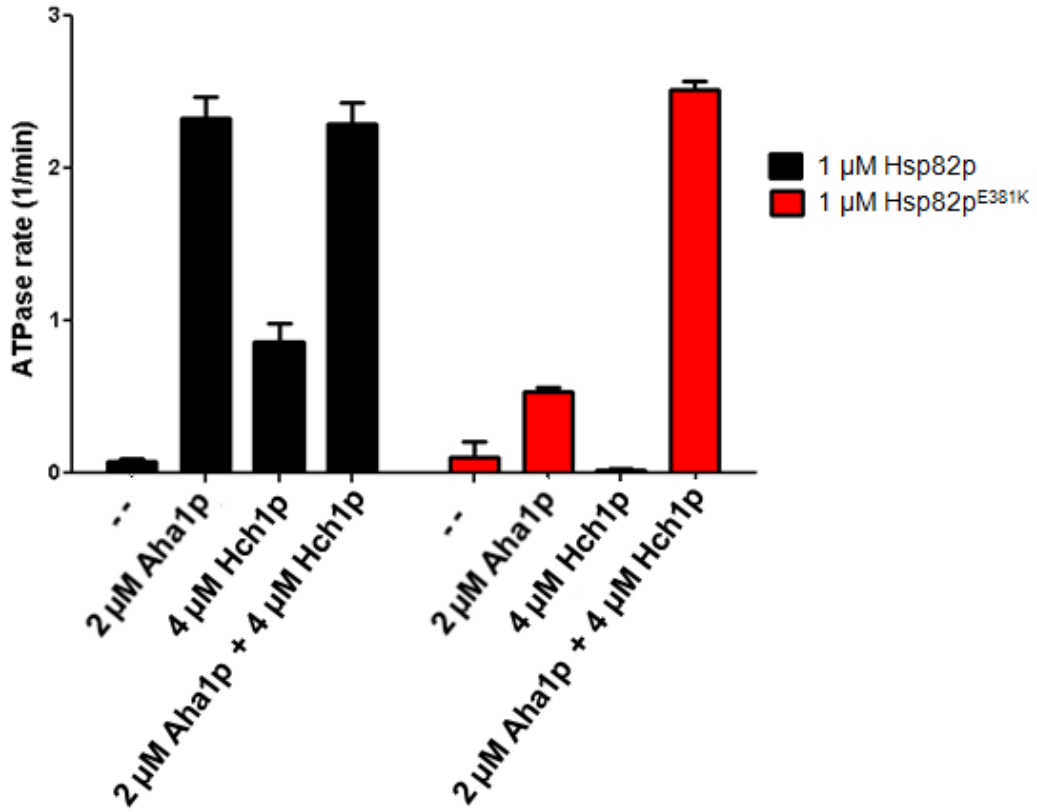

FIGURE 3.8: Effect of older purified Hch1p on the stimulated and non-stimulated rate of Hsp82p, and Hsp82p^{E381K}

A representative ATPase experiment was conducted with Hsp82p [81] and Hsp82p^{E381K} (red). 1 µM of Hsp82p, or Hsp82p^{E381K} was used. The ATPase rate was measured at a permissive temperature (30°C). Both the intrinsic and stimulated rate (2 µM Aha1p) of the Hsp82p, and Hsp82p^{E381K} was measured with or without 4 µM Hch1p. The Hch1p tested was from an older preparation

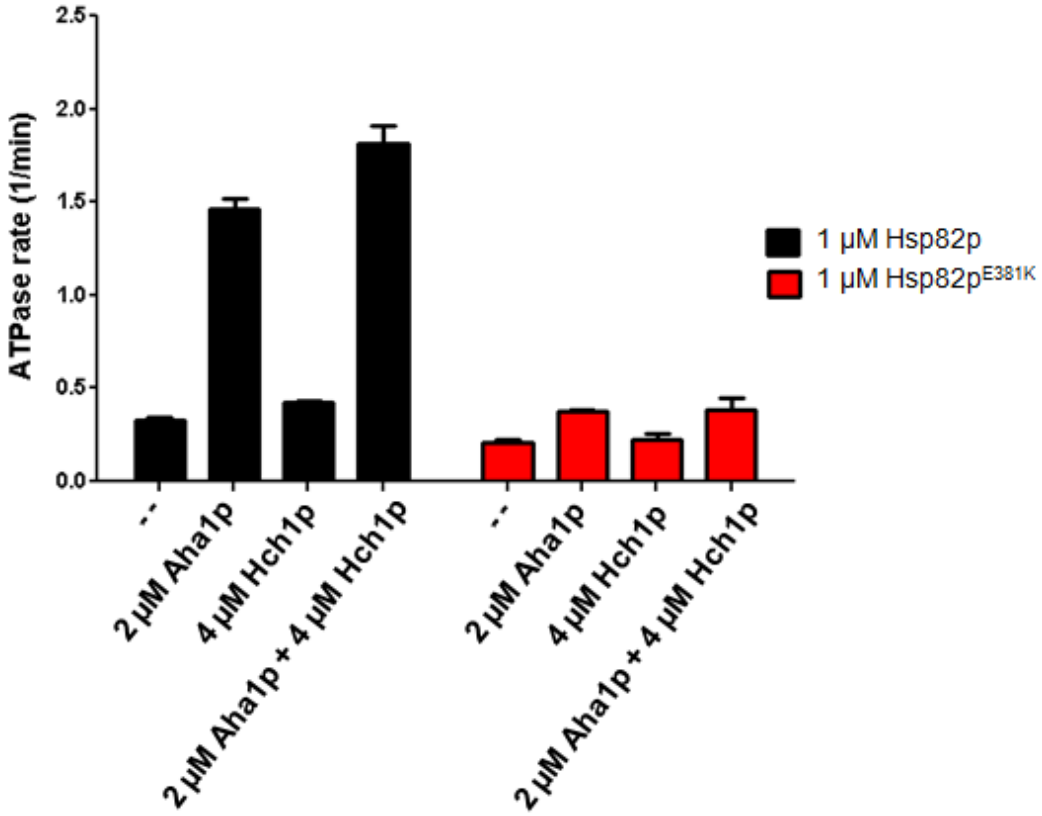

FIGURE 3.9: Effect of newer purified Hch1p on the stimulated and non-stimulated rate of Hsp82p, and Hsp82p^{E381K}

A representative ATPase experiment was conducted with Hsp82p [81] and Hsp82p^{E381K} (red). 1 µM of Hsp82p, or Hsp82p^{E381K} was used. The ATPase rate was measured at a permissive temperature (30°C). Both the intrinsic and stimulated rate (2 µM Aha1p) of the Hsp82p, and Hsp82p^{E381K} was measured with or without 4 µM Hch1p. The Hch1p tested was from a newer preparation.

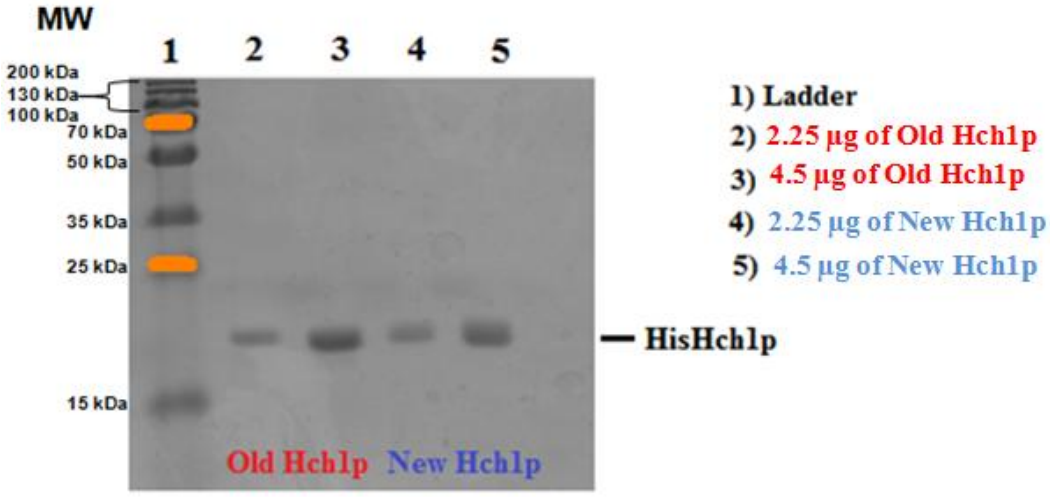

FIGURE 3.10: SDS-PAGE gel of both Hch1p purified samples used in experiments

Protein samples were resolved by SDS-PAGE (15% with a 8% stacking gel) and stained with commassie to visulaize protein

Chapter 4

Discussion

For the purpose of this study, I focused only on characterizing the ATPase activity three of the many Hsp82p mutants: Hsp82p^{A587T}, Hsp82p^{G313S}, and Hsp82p^{E381K}.

4.1 The Characterization of Hsp82pA587T

When I first characterized Hsp82p^{A587T}, I tested the intrinsic and stimulated rate of the mutant. Hsp82p^{A587T} had a lower intrinsic rate than the wild-type, but when Aha1p was added to the ATPase reaction the stimulated rate was significantly higher than the wild-type (18.5 and 4.7 folds respectively) (Figure 3.1B). Over stimulation by Aha1 could be the reason why we see a growth defect in yeast expressing Hsp82p^{A587T} at 37°C. When a cell is stressed at higher temperatures, the Hsp90 system including the co-chaperone proteins are upregulated and overexpressed. A possibility for why Hsp82p^{A587T} displays a temperature sensitive phenotype at 37°C is in the presence of an increased Aha1p concentration Hsp82p^{A587T} ATPase is hyper stimulated. The chaperone adopts the closed ATP hydrolyzing conformation too often for Hsp82p^{A587T} to properly function.

I also characterised the Hsp82p^{A587T} mutant with two other co-chaperone proteins, Sti1p and Sba1p. Both Sti1p and Sba1p inhibit the stimulated ATPase rate of Hsp82p^{A587T} similarly to that of the wild-type. Previous literature has shown that the over expression of Sti1p corrected the temperature sensitive growth phenotype seen in yeast expressing Hsp82p^{A587T} (Figure 4.1) [83]. Another study done by Johnson *et. al* suggested that the Hsp82p^{A587T} dependency

on Sti1p was not an issue with the mutant interacting with the co-chaperone [82]. Using the equivalent mutations of Hsp82p^{A587T} in the constitutively expressed Hsp82 (Hsc82p^{A583T}) the study demonstrated that a comparable amount of Sti1p was pulled down with the mutant and the wild-type (Figure 4.2). From these observations, I had hypothesized that the Hsp82p^{A587T} dependency on Sti1p was likely a result of the co-chaperone not inhibiting the mutants effectively. I had predicted that Sti1p would not inhibit the ATPase activity of the Hsp82p^{A587T} mutant to the same extent that it inhibited the wild-type. Surprisingly, when I tested the Sti1p inhibition of Hsp82p^{A587T}, I found that the inhibition of the mutant by Sti1p was similar to that of the wild-type (Figure 3.4).

When conducting simplified *in vitro* assays, there are limitations to studying complex systems, such as the Hsp90 system. *In vivo* there are as many as 20-30 co-chaperones, and hundreds of client proteins that can interact with Hsp82p. The ATPase assays conducted in my study had a very limited selection of proteins in the reaction – at most, we tested Hsp82p with three other co-chaperones in one reaction. Essentially, *in vitro*, we are limiting the binding partners/co-chaperones that Hsp82p can interact with, which allows us to specifically study interactions of interest; Hsp82p behavior in the cell is much more complicated. Johnson *et. al* had demonstrated that the Hsc82p^{A583T} mutant had no trouble binding to Sti1p [82]. The inhibition of Hsp82p^{A587T} by Sti1p observed could be an artificial result. There is also the possibility that Sti1p has difficulty inhibiting Hsp82p^{A587T} properly *in vivo* because the interaction is inhibited by the chaperone relationship with a client protein or another co-

chaperone. This would explain why the over expression of Sti1p rescues the Hsp82p^{A587T} mutant growth phenotype seen in the experiment conducted by Chang *et. al* (Figure 4.1) [83]. In this situation, *in vivo* assays would be more informative than the enzyme-linked assays that I conducted, but recreating an environment that mimics the cell *in vivo* is beyond the scope of my study.

Another theory for the rescue of the Hsp82p^{A587T} mutant growth phenotype by the overexpression of Sti1p could be linked to the hyper stimulated ATPase activity when Aha1p interacts with Hsp82p^{A587T} [83]. As previously mentioned, one of the possible problems with Hsp82p^{A587T} could be an extreme sensitivity to Aha1p stimulation, which implies that it adopts the closed/N-terminal dimerization form too often. Sti1p has the opposite effect of Aha1p on Hsp90, and prevents the closed conformation. The overexpression of Sti1p would result in more "early" Hsp90 complexes and correct the over stimulation by Aha1p. In my assay, not only did I limit the binding partners/co-chaperones that Hsp82p can interact with, I also accounted for different binding affinities of each co-chaperone and used concentrations that ensured that Hsp82p had equal chances of binding to each chaperone(s) - essentially skewing the dynamics that would normally be found *in vivo.* In this study I was only concerned about the overall characterization of the mutants ATPase rate, but other experiments could be done to better mimic *in vivo* conditions. An example of future experiments could be done is to first analyze chaperone and co-chaperone levels during permissive and non-permissive conditions *in vivo*, and then tailoring my assay concentrations *in vitro* to mimic this.

The last co-chaperone that I used in the characterization of the Hsp82p^{A587T} mutant was Sba1p. Like Sti1p, Sba1p also inhibits the ATPase activity of Hsp90 but not as robustly. In the previously discussed study done by Johnson *et. al*, it was also demonstrated that Sba1p did not interact with the Hsc82p^{A583T} mutant as the co-chaperone was not found in a pull down with Hsc82p^{A583T} (Figure 4.2) [82]. Assuming that Hsc82p^{A583T} has difficulty binding with Sba1p, I had predicted that Sba1p would not inhibit Hsp82p^{A587T}. When I tested the Sba1 inhibition of the Hsp82p^{A587T} mutant, I found the inhibition to be very similar to that of the wild-type (Figure 3.6). This implies that there is no issue with Sba1p ability to bind/interacting with the Hsp82p^{A587T} mutant. Once again this could be an artificial result of my assay, as I limited the proteins in the assay, and used concentrations that skewed co-chaperone binding affinities to Hsp82p. To investigate if Sba1p had a lower binding affinity to Hsp82p^{A587T} compared to the wild-type, it would be informative to conduct an experiment where Sba1p is titrated at different concentrations into a stimulated reaction. This titration experiment could also be conducted with Sti1p to test the binding affinity of the co-chaperone with Hsp82p^{A587T}.

For my study I had assumed that both the constitutive and the inducible forms of yeast Hsp90, Hsc82p and Hsp82p respectively, were functionally equivalent and only differed in their transcriptional regulation and levels of expression [3,84,85]. It would be interesting to explore if there was a difference between the constitutive and the inducible forms of yeast Hsp90 in either co-chaperone affinity, or ATPase activities.

4.2 The Characterization of Hsp82pG313S

We showed that both Hsp82p^{G313S} and Hsp82p^{A587T} mutants were rescued by the deletion of *HCH1* (Figure 1.10). From this observation I had hypothesized that the molecular defects of both Hsp82p^{G313S} and Hsp82p^{A587T} were similar. The findings by Chang *et al*., that the over expression of Sti1p rescued the growth phenotype of both Hsp82p^{G313S} and Hsp82p^{A587T}, supported this hypothesis. When I tested the intrinsic and stimulated rate of the Hsp82p^{G313S}, I found the mutant had a lower intrinsic rate then the wild-type, and that this rate could not be robustly stimulated by Aha1. Our assay was not sensitive enough to measure the low ATPase rate of Hsp82p^{G313S} – in this case the signal to noise ratio was very low and we could not conclude about the properties of Hsp82p^{G313S}.

Although I was unable to characterize the Hsp82p^{G313S} mutant due to low signal to noise ratio, this issue with the mutant highlighted the fact that all my experiments were missing a very important control. I had erroneously assumed that the ATPase activity observed in all my experiments and conditions was due exclusively to either Hsp82p or the mutants. I should have conducted a control where I did the ATPase assay with an Hsp82p inhibitor present. Inhibitors of Hsp82p are very specific and effective; this would allow me to confirm if any of the ATPase activity observed is due to a contaminating ATPase. Lacking a proper control to limit the background noise of contaminating ATPases, no conclusive conclusions can be drawn about the relationships between the co-chaperones and the mutants. My data can only be used to suggest a relationship, and the experiments will need to be redone.

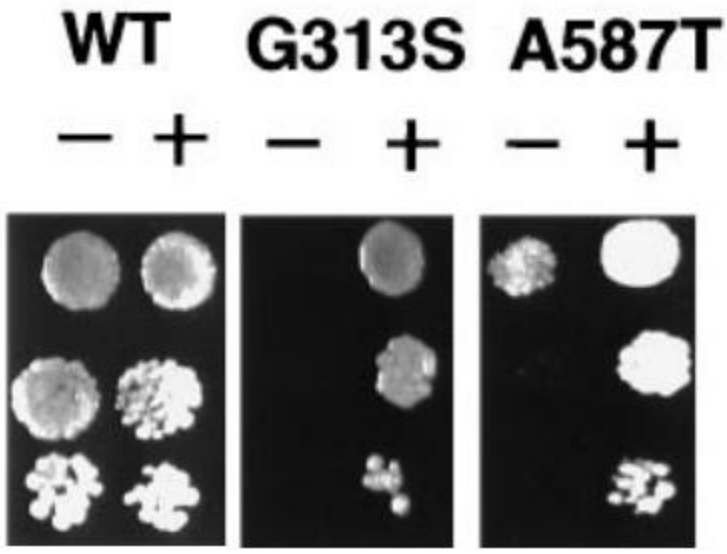

FIGURE 4.1: Overexpression of STI1 in wild-type Hsp82p, and Hsp82p^{G313S}, and Hsp82p^{A587T} cells

A growth assay of wild-type Hsp82p, Hsp82p^{G313S}, and Hsp82p^{A587T} strains with or without a multicopy *STI1* expression plasmid grown on YPDA media at 35°C and 36°C respectively. Figure from [83].

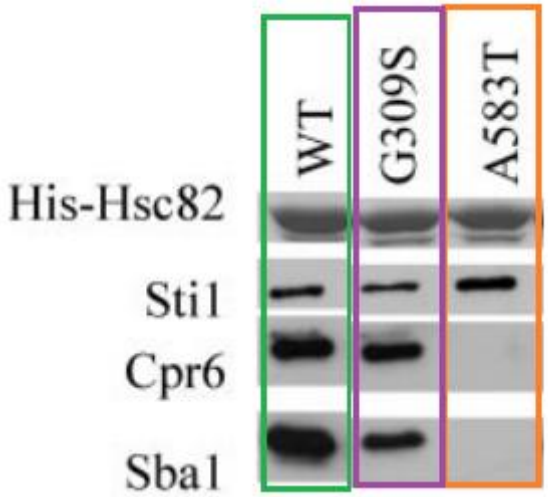

FIGURE 4.2: Proteomic Analysis of wild-type, G309S, and A583T mutants with STI1, SBA1, and CRP6

Commassie stain and Western blots of cell lysates from pulldown of Hsc82(green), $Hsc82^{G309S}$ (purple), and Hsc^{A583T} (orange). Complex were isolated using nickel bound beads, the upper panels was stained by commassie to visualize the His-Hsc82p present, while the lower panels were probed for the Sti1p, Sba1p, and Cpr6. Figure from [82].

4.3 The Characterization of Hsp82pE381K

I was particularly interested in the Hsp82p^{E381K} mutant because the temperature sensitive growth phenotype is rescued by the overexpression of Hch1p (Figure 1.7) [76]. When we tested the intrinsic and stimulated rate of Hsp82p^{E381K}, I found the mutant had a similar intrinsic rate, but was unable to achieve the same level of Aha1p mediated stimulation as the wild-type (Figure 3.1A). I also tested the effect of Hch1p on the Aha1p stimulated rate of both the wild-type and the Hsp82p^{E381K} mutant. At first, I found that with Hch1p we saw a rescue in the Aha1p stimulated ATPase rate of Hsp82p^{E381K} to wild-type Aha1p stimulated ATPase activity levels (Figure 3.7). Unfortunately, the result was not reproducible when this experiment was repeated with a different sample of Hch1p that was purified after the original sample was depleted. I found that this new Hch1p did not rescue the Hsp82p^{E381K} Aha1p stimulated ATPase rate (Figure 3.8). After testing both samples in an attempt to discern a reason for the drastically different results and yielding explanation, I had to accept the reproducible trend that I observed with the newer Hch1p.

In characterizing the ATPase activity of Hsp82p^{E381K}, I also found that the Hsp82p^{E381K} low Aha1p stimulated rate could not be inhibited by Sti1p (Figure 3.5). This data corresponded with previous studies looking at the relationship between Sti1p and Hsp82p^{E381K}. The study done by Johnson *et. al* supported my findings as the proteomics data shows the equivalent Hsc82p^{E377K} mutant only weakly associates to Sti1p (Figure 4.3) [2]. This suggested that the Sti1p had difficulty binding/interacting with the Hsp82p^{E381K} mutant. To test this, I could

once again use a titration assay with varying concentrations of Sti1p added to an Hsp82p^{E381K} Aha1p stimulated reaction.

4.4 Summary

In summary I was able to characterize the ATPase activity of Hsp82p^{A587T} and Hsp82p^{E381K} mutant. What I found was that the Hsp82p^{A587T} mutant were over stimulated by Aha1p, but had a similar relationship as the wild-type Hsp82p in terms of the Sti1p and Sba1p. With the Hsp82p^{E381K} mutant I observed that the mutant was not stimulated robustly by Aha1p, and this stimulated rate was not inhibited by Sti1p. Due to the low signal to noise ratio I was unable to characterize the Hsp82p^{G313S} mutant.

I was also unable to discover a novel function for the co-chaperone Hch1p. Future experiments with need to be done or repeated with the new Hch1p preparation that showed reproducible results. Expermients will also need to be redone with a control that contains a Hsp82p specific inhibitor to eliminate the background noise, and ensure that the ATPase activity seen is a result of Hsp82p, or the Hsp82p mutants.

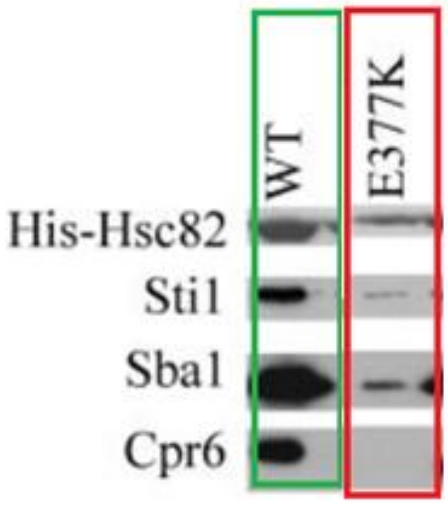

Figure 4.3 : Proteomic Analysis of wild-type and mutant interactions with STI1, SBA1, and CPR6

Commassie stain and Western blots of cell lysates from pulldown of His-Hsc82 (green), and Hscp^{E377K} (red).The mutant cells was co-expressed with untagged wild-type. Complexes were isolated using nickle bound beads, the upper panels was stained by Coommassie to visulaize the HisHsc82p present, while the lower panels were probed for the Sti1p, Sba1p, and Cpr6. Figure from [82].

Chapter 5

References

1. Anfinsen CB (1973) Principles that govern the folding of protein chains. Science 181: 223-230.
2. Nathan DF, Vos MH, Lindquist S (1997) In vivo functions of the Saccharomyces cerevisiae Hsp90 chaperone. Proc Natl Acad Sci U S A 94: 12949-12956.
3. Borkovich KA, Farrelly FW, Finkelstein DB, Taulien J, Lindquist S (1989) hsp82 is an essential protein that is required in higher concentrations for growth of cells at higher temperatures. Mol Cell Biol 9: 3919-3930.
4. Ellis RJ (2001) Macromolecular crowding: obvious but underappreciated. Trends Biochem Sci 26: 597-604.
5. Wegele H, Muller L, Buchner J (2004) Hsp70 and Hsp90--a relay team for protein folding. Rev Physiol Biochem Pharmacol 151: 1-44.
6. Nathan DF, Lindquist S (1995) Mutational Analysis of Hsp90 Function: Interaction with a Steroid Receptor and a Protein Kinase. Molecular and Cellular Biology 15: 3917-3925.
7. Lai BT, Chin NW, Stanek AE, Keh W, Lanks KW (1984) Quantitation and intracellular localization of the 85K heat shock protein by using monoclonal and polyclonal antibodies. Mol Cell Biol 4: 2802-2810.
8. Welch WJ, Feramisco JR (1982) Purification of the major mammalian heat shock proteins. J Biol Chem 257: 14949-14959.
9. Wandinger SK, Richter K, Buchner J (2008) The Hsp90 Chaperone Machinery. Journal of Biological Chemistry 283: 18473-18477.
10. Chen B, Zhong D, Monteiro A (2006) Comparative genomics and evolution of the HSP90 family of genes across all kingdoms of organisms. BMC Genomics 7: 156.
11. Mayer MP, Bukau B (2005) Hsp70 chaperones: cellular functions and molecular mechanism. Cell Mol Life Sci 62: 670-684.
12. Buchner J (1999) Hsp90 & Co. - a holding for folding. Trends Biochem Sci 24: 136-141.
13. Wandinger SK, Richter K, Buchner J (2008) The Hsp90 chaperone machinery. J Biol Chem 283: 18473-18477.
14. Wiech H, Buchner J, Zimmermann R, Jakob U (1992) Hsp90 chaperones protein folding *in vitro*. Nature 358: 169-170.
15. Freeman BC, Morimoto R (1996) The human cytosolic molecular chaperone hsp90, hsp70 (hsc70) and hdj-1 have distinct roles in recognition of a non-native protein and proteon folding. EMBO J 15: 2969-2979.
16. Holt SE, Aisner DL, Baur J, Tesmer VM, Dy M, et al. (1999) Functional requirement of p23 and Hsp90 in telomerase complexes. Genes Dev 13: 817-826.
17. Keppler BR, Grady AT, Jarstfer MB (2006) The biochemical role of the heat shock protein 90 chaperone complex in establishing human telomerase activity. J Biol Chem 281: 19840-19848.

18. Harst A, Lin H, Obermann WM (2005) Aha1 competes with Hop, p50 and p23 for binding to the molecular chaperone Hsp90 and contributes to kinase and hormone receptor activation. Biochemistry Journal: 789-797.
19. McClellan AJ, Xia Y, Deutschbauer AM, Davis RW, Gerstein M, et al. (2007) Diverse cellular functions of the Hsp90 molecular chaperone uncovered using systems approaches. Cell 131: 121-135.
20. Neckers L (2002) Hsp90 inhibitors as novel cancer chemotherapeutic agents. Trends in Molecular Medicine 8.
21. Bild AH, Yao G, Chang JT, Wang Q, Potti A, et al. (2006) Oncogenic pathway signatures in human cancers as a guide to targeted therapies. Nature 439: 353-357.
22. Pearl LH, Prodromou C (2006) Structure and Mechanism of the Hsp90 Molecular Chaperone Machinery. The Annual Review of Biochemistry 75: 271-294.
23. Richter K, Hendershot LM, Freeman BC (2007) The cellular world according to Hsp90. Nat Struct Mol Biol 14: 90-94.
24. Bracher A, Hartl FU (2006) Hsp90 structure: when two ends meet. Nat Struct Mol Biol 13: 478-480.
25. Wayne N, Bolon DN (2007) Dimerization of Hsp90 Is Required for in Vivo Function: DESIGN AND ANALYSIS OF MONOMERS AND DIMERS. Journal of Biological Chemistry 282: 35386-35395.
26. Richter K (2001) Coordinated ATP Hydrolysis by the Hsp90 Dimer. Journal of Biological Chemistry 276: 33689-33696.
27. Allan RK, Ratajczak T (2011) Versatile TPR domains accommodate different modes of target protein recognition and function. Cell Stress Chaperones 16: 353-367.
28. Scheufler C, Brinker A, Bourenkov G, Pegoraro S, Moroder L, et al. (2000) Structure of TPR Domain–Peptide Complexes. Cell 101: 199-210.
29. Prodromou C, Siligardi G, R. OB, Woolfson DN, Regan L, et al. (1999) Regulation of Hsp90 ATPase activity by tetratricopeptide repeat (TPR)-domain co-chaperones. The EMBO Journal 18: 754-762.
30. Bishop SC, Burlison JA, Blagg BS (2007) Hsp90: a novel target for the disruption of multiple signaling cascades. Curr Cancer Drug Targets 7: 369-388.
31. Hawle P, Siepmann M, Harst A, Siderius M, Reusch HP, et al. (2006) The Middle Domain of Hsp90 Acts as a Discriminator between Different Types of Client Proteins. Molecular and Cellular Biology 26: 8385-8395.
32. Lotz GP (2003) Aha1 Binds to the Middle Domain of Hsp90, Contributes to Client Protein Activation, and Stimulates the ATPase Activity of the Molecular Chaperone. Journal of Biological Chemistry 278: 17228-17235.
33. Meyer P, Prodromou C, Hu B, Vaughan C, Roe SM, et al. (2003) Structural and functional analysis of the middle segment of hsp90: implications for ATP hydrolysis and client protein and cochaperone interactions. Mol Cell 11: 647-658.

34. Hainzl O, Lapina MC, Buchner J, Richter K (2009) The charged linker region is an important regulator of Hsp90 function. J Biol Chem 284: 22559-22567.
35. Tsutsumi S, Mollapour M, Prodromou C, Lee CT, Panaretou B, et al. (2012) Charged linker sequence modulates eukaryotic heat shock protein 90 (Hsp90) chaperone activity. Proc Natl Acad Sci U S A 109: 2937-2942.
36. Gooljarsingh LT, Fernandes C, Yan K, Zhang H, Grooms M, et al. (2006) A biochemical rationale for the anticancer effects of Hsp90 inhibitors: slow, tight binding inhibition by geldanamycin and its analogues. Proc Natl Acad Sci U S A 103: 7625-7630.
37. Workman P (2004) Combinatorial attack on multistep oncogenesis by inhibiting the Hsp90 molecular chaperone. Cancer Lett 206: 149-157.
38. Schliwa M, Woehlke G (2003) Molecular motors. Nature 422: 759-765.
39. Flom G (2005) Effect of Mutation of the Tetratricopeptide Repeat and Asparatate-Proline 2 Domains of Sti1 on Hsp90 Signaling and Interaction in Saccharomyces cerevisiae. Genetics 172: 41-51.
40. Prodromou C, Panaretou B, Chohan S, Siligardi G, O'Brien R, et al. (2000) The ATPase cycle of Hsp90 drives a molecular 'clamp' via transient dimerization of the N-terminal domains. EMBO J 19: 4383-4392.
41. Mickler M, Hessling M, Ratzke C, Buchner J, Hugel T (2009) The large conformational changes of Hsp90 are only weakly coupled to ATP hydrolysis. Nature Structural & Molecular Biology 16: 281-286.
42. Ratzke C, Berkemeier F, Hugel T (2012) Heat shock protein 90's mechanochemical cycle is dominated by thermal fluctuations. Proc Natl Acad Sci U S A 109: 161-166.
43. Richter K, Walter S, Buchner J (2004) The Co-chaperone Sba1 Connects the ATPase Reaction of Hsp90 to the Progression of the Chaperone Cycle. Journal of Molecular Biology 342: 1403-1413.
44. Siligardi G, Hu B, Panaretou B, Piper PW, Pearl LH, et al. (2004) Co-chaperone Regulation of Conformational Switching in the Hsp90 ATPase Cycle. Journal of Biological Chemistry 279: 51989-51998.
45. Pratt WB, Toft DO (2003) Regulation of signaling protein function and trafficking by the hsp90/hsp70-based chaperone machinery. Exp Biol Med (Maywood) 228: 111-133.
46. Pratt WB, Toft DO (1997) Steroid receptor interactions with heat shock protein and immunophilin chaperones. Endocr Rev 18: 306-360.
47. Catelli MG, Binart N, Jung-Testas I, Renoir JM, Baulieu EE, et al. (1985) The common 90-kd protein component of non-transformed '8S' steroid receptors is a heat-shock protein. EMBO J 4: 3131-3135.
48. Siligardi G, Hu B, Panaretou B, Piper PW, Pearl LH, et al. (2004) Co-chaperone regulation of conformational switching in the Hsp90 ATPase cycle. J Biol Chem 279: 51989-51998.
49. Wandinger SK, Suhre MH, Wegele H, Buchner J (2006) The phosphatase Ppt1 is a dedicated regulator of the molecular chaperone Hsp90. EMBO J 25: 367-376.

50. Li J, Soroka J, Buchner J (2012) The Hsp90 chaperone machinery: Conformational dynamics and regulation by co-chaperones. Biochim Biophys Acta 1823: 624-635.
51. Caplan AJ (2003) What is a co-chaperone? Cell Stress Chaperones 8: 105-107.
52. Chen MS, Silverstein AM, Pratt WB, Chinkers M (1996) The tetratricopeptide repeat domain of protein phosphatase 5 mediates binding to glucocorticoid receptor heterocomplexes and acts as a dominant negative mutant. J Biol Chem 271: 32315-32320.
53. Riggs DL, Cox MB, Cheung-Flynn J, Prapapanich V, Carrigan PE, et al. (2004) Functional specificity of co-chaperone interactions with Hsp90 client proteins. Crit Rev Biochem Mol Biol 39: 279-295.
54. Prodromou C, Siligardi G, O'Brien R, Woolfson DN, Regan L, et al. (1999) Regulation of Hsp90 ATPase by tetraicopetide repeat (TPR)-domain co-chaperone EMBO J 18: 754-762.
55. Morishima Y (2003) The Hsp90 Cochaperone p23 Is the Limiting Component of the Multiprotein Hsp90/Hsp70-based Chaperone System in Vivo Where It Acts to Stabilize the Client Protein{middle dot}Hsp90 Complex. Journal of Biological Chemistry 278: 48754-48763.
56. Richter K, Muschler P, Hainzl O, Reinstein J, Buchner J (2003) Sti1 is a non-competitive inhibitor of the Hsp90 ATPase. Binding prevents the N-terminal dimerization reaction during the atpase cycle. J Biol Chem 278: 10328-10333.
57. Harst A (2005) Aha1 competes with Hop, p50, p23, for binding to the molecuar chaperone Hsp90 and contributes to Kinase and hormone receptor activation Biochemical Journal 387: 789-796.
58. Li J, Richter K, Buchner J (2011) Mixed Hsp90-cochaperone complexes are important for the progression of the reaction cycle. Nat Struct Mol Biol 18: 61-66.
59. Johnson JL, Halas A, Flom G (2007) Nucleotide-dependent interaction of Saccharomyces cerevisiae Hsp90 with the cochaperone proteins Sti1, Cpr6, and Sba1. Mol Cell Biol 27: 768-776.
60. Morishima Y, Kanelakis KC, Murphy PJ, Lowe ER, Jenkins GJ, et al. (2003) The hsp90 cochaperone p23 is the limiting component of the multiprotein hsp90/hsp70-based chaperone system in vivo where it acts to stabilize the client protein: hsp90 complex. J Biol Chem 278: 48754-48763.
61. Grad I, McKee TA, Ludwig SM, Hoyle GW, Ruiz P, et al. (2006) The Hsp90 cochaperone p23 is essential for perinatal survival. Mol Cell Biol 26: 8976-8983.
62. Fang Y, Fliss A, Rao J, Caplan A (1998) SBA1 encodes a yeast Hsp90 Cochaperone that is Homologous to Vertebrate p23 protiens. Molecular and Cellular Biology 18: 3727-3734
63. Ali M, Roe SM, Vaughan CK, Meyer P, Panaretou B, et al. (2006) Crystal structure of an Hsp90– nucleotide–p23/Sba1 closed chaperone complex. Nature Publishing Group 440: 1013-1017.

64. Bose S, Weikl T, Bugl H, Buchner J (1996) Chaperone function of Hsp90-associated proteins. Science 274: 1715-1717.
65. Freeman BC, Toft DO, Morimoto RI (1996) Molecular chaperone machines: chaperone activities of the cyclophilin Cyp-40 and the steroid aporeceptor-associated protein p23. Science 274: 1718-1720.
66. Lotz GP, Lin H, Harst A, Obermann WM (2003) Aha1 binds to the middle domain of Hsp90, contributes to client protein activation, and stimulates the ATPase activity of the molecular chaperone. J Biol Chem 278: 17228-17235.
67. Retzlaff M, Hagn F, Mitschke L, Hessling M, Gugel F, et al. (2010) Asymmetric activation of the hsp90 dimer by its cochaperone aha1. Mol Cell 37: 344-354.
68. Ali MM, Roe SM, Vaughan CK, Meyer P, Panaretou B, et al. (2006) Crystal structure of an Hsp90-nucleotide-p23/Sba1 closed chaperone complex. Nature 440: 1013-1017.
69. Holt SE, Aisner DL, Baur J, Tesmer VM, Dy M, et al. (1999) Functional requirement of p23 and Hsp90 in telomerase complexes. Genes & Development 13: 817-826.
70. Panaretou B, Siligardi G, Meyer P, Maloney A, Sullivan JK, et al. (2002) Activation of the ATPase activity of hsp90 by the stress-regulated cochaperone aha1. Mol Cell 10: 1307-1318.
71. Meyer P, Prodromou C, Liao C, Hu B, Roe SM, et al. (2004) Structural basis for recruitment of the ATPase activator Aha1 to the Hsp90 chaperone machinery. EMBO J 23: 8.
72. Nathan D, Vos MH, Lindquist S (1999) Identification of SSF1, CNS1, and HCH1 as multicopy suppressors of a Saccharomyces cerevisiae Hsp90 loss-of-function mutation. Proc Natl Acad Sci USA 96: 1409-1414.
73. Retzlaff M, Hagn F, Mitschke L, Hessling M, Gugel F, et al. (2010) Asymmetric Activation of the Hsp90 Dimer by Its Cochaperone Aha1. Molecular Cell 37: 344-354.
74. Koulov AV, LaPointe P, Lu B, Razvi A, Coppinger J, et al. (2010) Biological and Structural Basis for Aha1 Regulation of Hsp90 ATPase Activity in Maintaining Proteostasis in the Human Disease Cystic Fibrosis. Molecular Biology of the Cell 21: 871-884.
75. Zhao R, Houry WA (2007) Molecular interaction network of the Hsp90 chaperone system. Adv Exp Med Biol 594: 27-36.
76. Nathan DF, Vos MH, Lindquist S (1999) Identification of SSF1, CNS1, and HCH1 as multicopy suppressors of a Saccharomyces cerevisiae Hsp90 loss-of-function mutation. Proc Natl Acad Sci U S A 96: 1409-1414.
77. Panaretou B, Prodromou C, Roe SM, O'Brien R, Ladbury JE, et al. (1998) ATP binding and hydrolysis are essential to the function of the Hsp90 moleculat chaperone *in vivo*. EMBO J 17: 4829-4836
78. Obermann WM, Sondermann H, Russo AA, Pavletich NP, Hartl FU (1998) In vivo function of Hsp90 is dependent on ATP binding and ATP hydrolysis. J Cell Biol 143: 901-910.

79. Singh M, Yadav A, Ma XL, Amoah E (2010) Plasmid DNA Transformation in Escherichia Coli: Effect of Heat Shock Temperature, Duration, and Cold Incubation of CaCl2 Treated Cells. International Journal of Biotechnology and Biochemistry 6 561–568
80. Prodromou C, Roe SM, O'Brien R, Ladbury JE, Piper PW, et al. (1997) Identification and structural characterization of the ATP/ADP-binding site in the Hsp90 molecular chaperone. Cell 90: 65-75.
81. Wu H, Blackledge M, Maciejewski MW, Mullen GP, King SM (2003) Relaxation-based structure refinement and backbone molecular dynamics of the dynein motor domain-associated light chain. Biochemistry 42: 57-71.
82. Johnson JL, Halas A, Flom G (2007) Nucleotide-Dependent Interaction of Saccharomyces cerevisiae Hsp90 with the Cochaperone Proteins Sti1, Cpr6, and Sba1. Molecular and Cellular Biology 27: 768-776.
83. Chang HJ, Nathan DF, Lindquist S (1997) In Vivo Analysis of Hsp90 CoChaperone Sti1 (p60)
Molecular and Cellular Biology 17: 318-325.
84. Cox MB, Miller CA, 3rd (2003) Pharmacological and genetic analysis of 90-kDa heat shock isoprotein-aryl hydrocarbon receptor complexes. Mol Pharmacol 64: 1549-1556.
85. Erkine AM, Szent-Gyorgyi C, Simmons SF, Gross DS (1995) The upstream sequences of the HSP82 and HSC82 genes of Saccharomyces cerevisiae: regulatory elements and nucleosome positioning motifs. Yeast 11: 573-580.